CHARACTERIZATION OF ADENOSINE NUCLEOSIDASE FROM ALASKA PEA SEEDS

by

Abdullah K. Shamsuddin

A Thesis Submitted to the
Faculty of the College of Graduate Studies at
Middle Tennessee State University
in Partial Fulfillment of
the Requirements for the Degree of
Master of Science
in Chemistry

Middle Tennessee State University

August 2015

Thesis Committee:

Dr. Paul C. Kline, Chair

Dr. Donald A. Burden

Dr. Kevin L. Bicker

I dedicate this research to my parents, my sisters, and my brother. I love you all.

ACKNOWLEDGEMENTS

I would like to express my sincere gratitude to my advisor, Dr. Paul C. Kline, for his guidance, support, and ongoing encouragement throughout this project. I also wish to thank my committee members, Dr. Donald A. Burden and Dr. Kevin L. Bicker, for their advice and insightful comments.

In addition, I would like to thank all the staff and faculty of the Department of Chemistry for their contribution to the success of this study.

Lastly, I wish to thank my family and my friends, without whom none of my accomplishments would have been possible. Thank you for you endless support, concern, love, and prayer.

ABSTRACT

Adenosine nucleosidase was purified from Alaska pea seeds five days after germination. A 4-fold purification has been reached with a 1.3 % recovery. The subunit molecular weight of adenosine nucleosidase was determined by mass spectrometry to be 26,103 daltons. The number of subunits was 1. The Michaelis constant, K_m, and the maximum velocity, V_{max}, for adenosine were determined to be 137 ± 48 μM, and 0.34 ± 0.02 μM/min respectively.

In addition, the substrate specificity of the enzyme was investigated. Based on the observed substrate specificity, adenosine nucleosidase from Alaska pea seeds belongs to the non-specific inosine-uridine nucleoside hydrolases (IU-NHs). An interesting finding was the fact that the purified enzyme was the only plant source that used 2', 3', and 5'-deoxyadenosine as substrates. This is completely different from the parasitic protozoa IU-NH, specifically the nucleoside hydrolase from C. *fasciculata*, which showed no activity toward deoxynucleosides. This difference also indicates that adenosine nucleosidase from Alaska pea goes through a different mechanism of reaction from that of parasitic protozoa. While these results provide insight about the enzyme from Alaska pea seeds, further conformation is required to support the statements above.

TABLE OF CONTENTS

Chapter III

RESULTS AND DISCUSSION

Chapter IV

REFERENCES

LIST OF TABLES

LIST OF FIGURES

CHAPTER I

INTRODUCTION

Nucleotides are important cellular components in plant metabolism, growth, and development. Catabolism of nucleotides result in the formation of nucleosides, which can undergo further degradation by nucleoside hydrolase to nucleobases. Nucleosides are intermediates of nucleotide metabolism. Nucleoside monophosphates (*e.g.* adenosine monophosphate AMP and uridine monophosphate UMP) are generated by nucleotide *de novo* synthesis (*1*). These monophosphates are further processed to all purine and pyrimidine nucleotides that are involved in many cellular reactions. Nucleotides are the structural subunits of nucleic acids. They consist of a cyclic furanoside-type sugar linked to a nitrogen-containing organic ring compound. In most nucleosides, the sugar is either ribose or deoxyribose, and the nitrogen-containing compound is either a purine or a pyrimidine (*1*). A nucleoside with one or more phosphate groups is called a nucleotide (Figure 1).

Purines and Pyrimidines

Purines and pyrimidines are two types of nitrogen-containing organic rings. Purines are aromatic compounds containing two heterocyclic rings with four nitrogen atoms, and they consist of a pyrimidine ring bonded to an imidazole ring. Pyrimidines, on the other hand, are aromatic organic compounds with only one heterocyclic ring containing two nitrogen atoms. Purines include adenine, guanine,

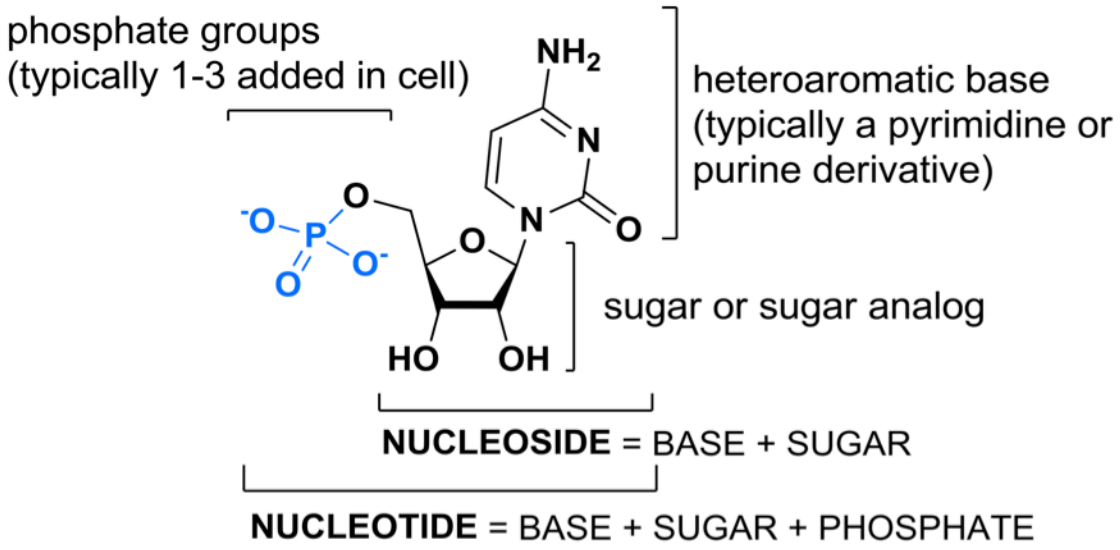

Figure 1. The structural elements of the nucleosides and nucleotides (*29*).

and hypoxanthine, which correspond to the nucleosides adenosine, guanosine, and inosine. Pyrimidines include cytosine, thymine, and uracil, which correspond to the nucleosides cytidine, thymidine, and uridine (Figure 2). Adenine, guanine, cytosine, and thymine are all found in DNA. In RNA however, thymine is replaced by uracil.

The processes of purine and pyrimidine metabolism in plants are important because they are essential for primary and secondary metabolism. They are also key in gene expression and play an important role in supporting many of the cellular and biochemical processes essential for cell growth (*1*). Purine and pyrimidine nucleotides are also central in information storage and recovery in dividing tissue cells. They perform this by acting as building blocks of DNA or DNA-synthesizing organelles (*2*). During photosynthesis and respiration, the purine nucleotide ATP is produced and used for

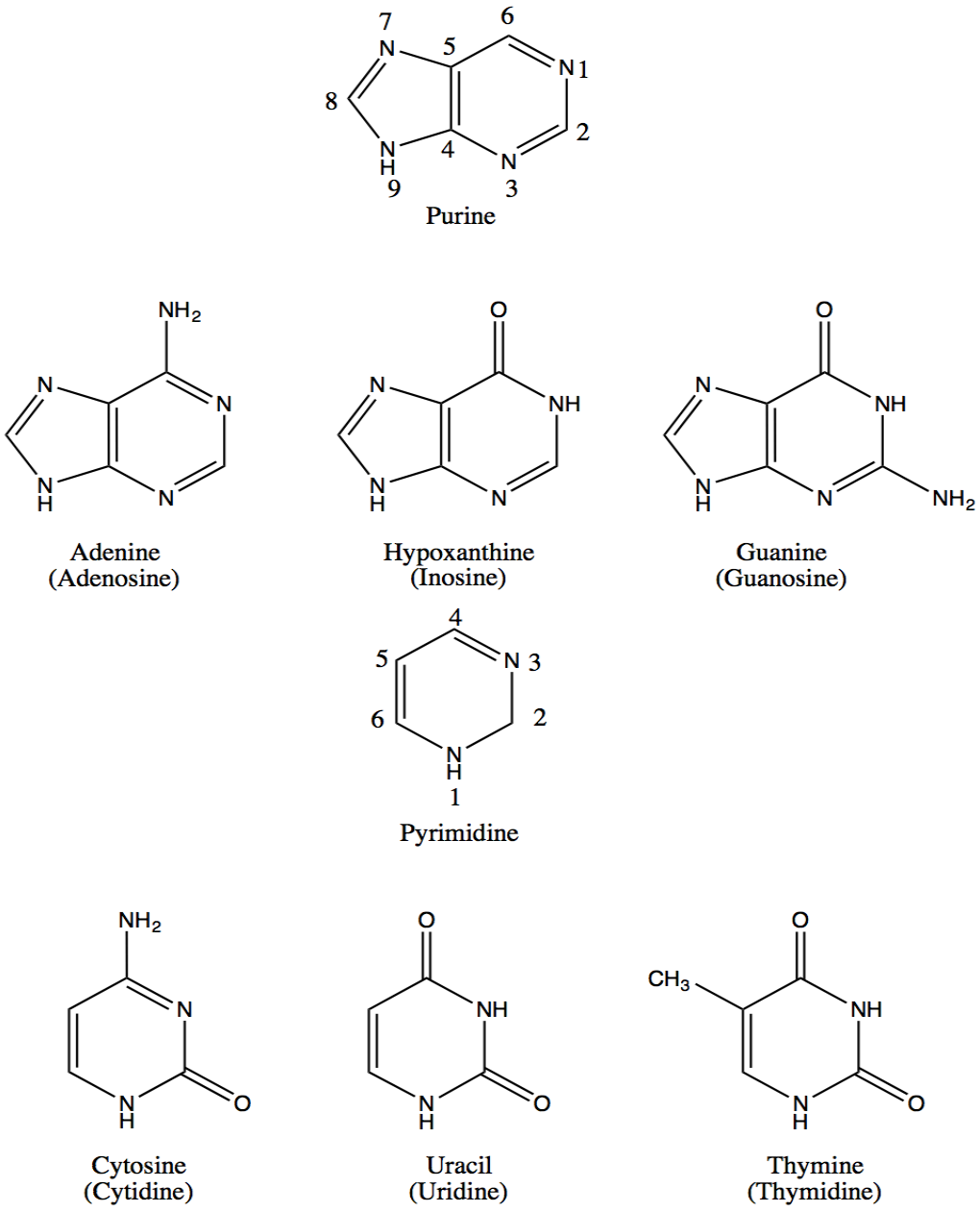

Figure 2. The common purine and pyrimidine bases with their numbering schemes.

general chemical energy conservation. The pyrimidine nucleotides have an important function as co-substrates (*3*).

Purine and Pyrimidine Metabolism

Nucleotide metabolism is divided into four pathways: *de novo* synthesis, nucleotide degradation, salvage pathways, and phosphotransfer reactions. Nucleotide metabolism is more complicated than amino acid metabolism, because the nucleotides and their intermediates are precursors for the synthesis of secondary metabolites and hormones (*1*). For example, UTP and UDP act as co-substrates and are directly involved in the synthesis and degradation of sucrose and UDP-glucose. UDP-glucose is the precursor for the synthesis of cellulose, glycoproteins, and phospholipids. Additionally, UDP-glucose acts as a glucosyl donor in the synthesis of secondary metabolites and hormones in a wide range of reactions that are catalyzed by the UDP-glucose glycosyltransferases family (*1*).

Pyrimidine nucleotide *de novo* biosynthesis, also called the orotate pathway, is defined as the formation of uridine monophosphate (UMP) from carbamoylphosphate (CP), aspartate, and 5-phosphoribosyl-1-pyrophosphate (PRPP). This pathway is made up of six enzymatic steps (Figure 3 steps 1– 6). The first step is the formation of carbamoylphosphate (CP), catalyzed by carbamoylphosphate synthase (CPSase) by the combination of carbonate, ATP, and an amino group from the side chain of glutamine. Aspartate transcarbamoylase (ATCase) then catalyzes the condensation of CP with aspartate to yield carbamoylaspartate (CA).

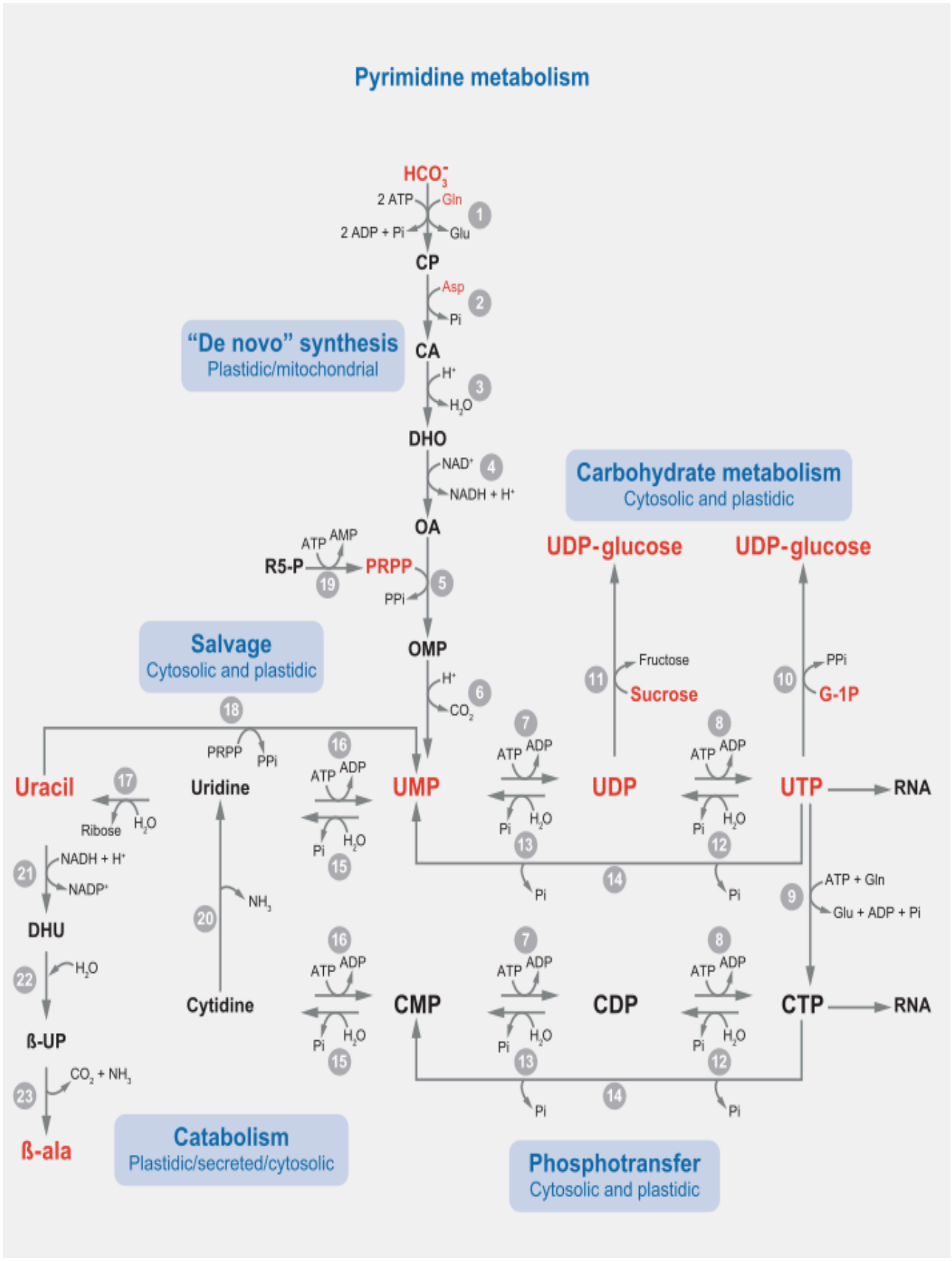
Pyrimidine metabolism
HCO3-
2 ATP
Gln
2 ADP + Pi
Glu
1
CP
Asp
2
Pi
"De novo" synthesis
Plastidic/mitochondrial
CA
H+
3
H2O
DHO
NAD+
4
NADH + H+
OA
Carbohydrate metabolism
Cytosolic and plastidic
ATP AMP
R5-P
PRPP
19
5
PPi
UDP-glucose
UDP-glucose
OMP
Salvage
Cytosolic and plastidic
H+
6
CO2
11
Fructose
Sucrose
10
PPi
G-1P
18
PRPP
PPi
16
ATP ADP
7
ATP ADP
8
ATP ADP
Uracil
17
Uridine
UMP
UDP
UTP
RNA
Ribose
H2O
Pi
H2O
Pi
H2O
Pi
H2O
13
12
21
NADH + H+
NADP+
14
Pi
Pi
9
ATP + Gln
Glu + ADP + Pi
DHU
20
NH3
22
H2O
16
ATP ADP
7
ATP ADP
8
ATP ADP
Cytidine
CMP
CDP
CTP
RNA
ß-UP
Pi
H2O
Pi
H2O
Pi
H2O
15
13
12
23
CO2 + NH3
14
Pi
Pi
ß-ala
Catabolism
Plastidic/secreted/cytosolic
Phosphotransfer
Cytosolic and plastidic

Figure 3. A general schematic outline of plant pyrimidine metabolism. The metabolic components shown are: 5-phosphoribosyl-1-pyrophosphate (*PRPP*), ribose-5-phosphate (*R5-P*), glutamine (*Gln*), glutamate (*Glu*), adenosine triphosphate (*ATP*), adenosine diphosphate (*ADP*), inorganic phosphate (*Pi*), carbamoyl phosphate (*CP*), carbamoyl aspartate (*CA*), dihydro-orotate (*DHO*), orotic acid (*OA*), orotidine 5' -monophosphate (*OMP*), uridine monophosphate (*UMP*), uridine diphosphate (*UDP*), uridine triphosphate (*UTP*), uridine diphosphoglucose (*UDP-glucose*), cytosine monophosphate (*CMP*), cytosine diphosphate (*CDP*), cytosine triphosphate (*CTP*), dihydrouracil (*DHU*), β-ureidopropionate (β -*UP*), β-alanine (β -*ala*), pyrophosphate (*PPi*), glucose-1-phosphate (*G-1P*), aspartate (*Asp*), and adenosine monophosphate (*AMP*). Reprinted from reference 1 with permission from Ann. Rev. Plant Biol. (2006).

The next step is the cyclization of carbamoylaspartate to produce the pyrimidine ring. This step is catalyzed by dihydroorotase (DHOase). Next, orotate (OA) is formed when dihydroorotate is oxidized by dihydroorotate dehydrogenase (DHODH). Orotate is attached to PRPP to produce orotidine 5'-monophosphate (OMP) and inorganic pyrophosphate by the enzyme orotate phosphoribosyltransferase (OPRTase). The last step involves decarboxylation of OMP by orotidylate decarboxylase (ODCase) to yield the final product, uridine-5'- monophosphate (UMP) (*1*).

The reactions in the pyrimidine nucleotide *de novo* synthesis pathway in plants take place in different subcellular locations (*1*). The first three steps take place in the plastid. The dehydrogenase reaction, where DHO is converted to OA, takes place in the inner mitochondrial membrane. However, the last two steps again occur in the plastid. Regulation of the *de novo* synthesis pathway is based on the enzymatic activity and is regulated via feedback and feedforward loops acting on CPSase and ATCase (*1*). The reactions of these enzymes were first observed in microbes and represent classic examples of allosteric regulation. Allosteric regulation of plant CPSase is accomplished by feedback inhibition with UMP and feedforward activation with PRPP. The feedback inhibition of CPSase by UMP can be overcome by ornithine.

Pyrimidine nucleotides are catabolized to pyrimidine nucleosides when a phosphate group is removed in the reaction catalyzed by 5'-nucleotidases (Steps 17, 20-23 of Figure 3). By removing the ribose group, the nucleosides are converted to free pyrimidine bases. This reaction is catalyzed by a group of nucleosidases that differ in their substrate specificity. Since plants and animals do not have cytosine deaminase, the

nucleoside cytidine is deaminated to uridine by cytidine deaminase (CDA), which is then metabolized to uracil (*1*). A reductive pathway degrades the bases uracil and thymine. There are three reactions in this pathway and they are catalyzed by dihydrouracil dehydrogenase (PYD1), dihydropyrimidinase (PYD2), and *β*-ureidopropionase (PYD3) (steps 21-23 of Figure 3) (*1*). The degradative pathway leads to the formation of *β*-alanine by releasing NH_3 and CO_2 (Figure 3).

The nucleotide *de novo* synthesis pathway consumes a lot of energy. Therefore, cells have established a strategy to reuse preformed nucleosides and nucleobases through the pyrimidine salvage pathway. The nucleosides thymine, uracil/cytosine are salvaged to their respective nucleotides via specific nucleoside kinases such as thymidine kinase and uridine kinase (*1*). Uracil is the only pyrimidine base that is directly salvaged with PRPP into UMP through uracil phosphoribosyltransferase (UPRT). To date, only one cDNA of UPRT from *Arabidopsis* has been cloned (*1*). UPRT was found to be structurally similar to phosphoribosyltransferases of other organisms and is located in the cytosol. Once completed, the *Arabidopsis* genome sequence revealed that small gene families encode UPRT and PRPP synthetase. Different members of the family are located either in the cytosol or the plastids. The expression data confirm that all isoforms are expressed differentially (*1*). From this result, it is assumed that the salvage pathway of pyrimidines take place in the plastids and the cytosol (*1*).

Purine nucleotides are synthesized through a *de novo* pathway from small molecules such as amino acids, glycine, glutamine, aspartate, 10-formyl tetrahydrofolate,

PRPP, and carbon dioxide (*1*). There are fourteen enzymatic reactions in the purine biosynthesis pathway (Figure 4).

Purine biosynthesis starts by forming phosphoribosylamine (PRA) from PRPP and glutamine, catalyzed by PRPP amidotransferase (ATase). Glycine amide ribonucleotide (GAR) is formed when a glycine is attached to PRA through an amide bond. This reaction is catalyzed by GRA synthetase (*1*). Using 10-formyltetrahydrofolate (10F-THF) as a source of carbon, the enzyme GAR transformylase (GART) transformylates GAR to formylglycinamide ribonucleotide (FGAR). ATP, glutamine and the enzyme formylglycinamidine ribonucleotide synthetase (FGAMS) are used to form formylglycinamidine ribonucleotide (FGAM).

5-aminoimidazole ribonucleotide (AIR) is formed when FGAM, catalyzed by AIR-synthase, goes through a ring closure (*1*). Since purines have two rings in their skeleton, CO_2, aspartate, and another molecule of 10F-THF are added to form the imidazole ring. AIR is then carboxylated to 4-carboxy aminoimidazole ribonucleotide (CAIR). The addition of aspartate in the next step forms *N*-succinyl-5-aminoimidazole-4-carboxamide ribonucleotide (SAICAR). The next step is catalyzed by adenylosuccinate lyase (ASL) and results in the release of fumarate to form 5-aminoimidazole-4-carboxamide ribonucleotide (AICAR).

The final carbon needed for the purine ring is provided by 10F-THF and 5-formaminoimidazole-4-carboxamide ribonucleotide (FAICAR) is formed. FAICAR undergoes dehydration and ring closure to form the first complete purine molecule inosine monophosphate (IMP) (*1*). After IMP, the purine biosynthesis pathway splits into

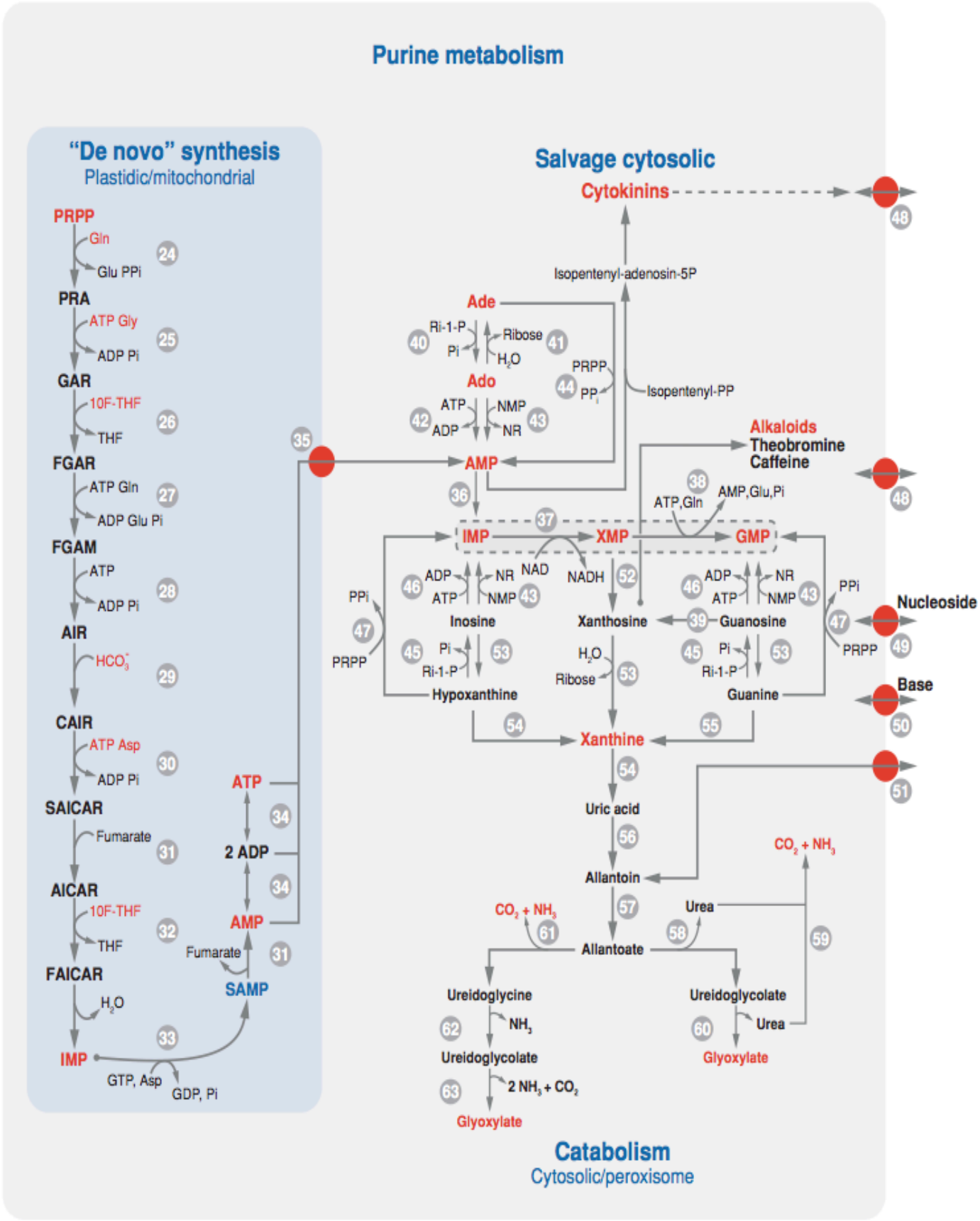
Purine metabolism
"De novo" synthesis
Plastidic/mitochondrial
PRPP
Gln
Glu PPi
PRA
ATP Gly
ADP Pi
GAR
10F-THF
THF
FGAR
ATP Gln
ADP Glu Pi
FGAM
ATP
ADP Pi
AIR
HCO3-
CAIR
ATP Asp
ADP Pi
SAICAR
Fumarate
AICAR
10F-THF
THF
FAICAR
H2O
IMP
GTP, Asp
GDP, Pi
ATP
2 ADP
AMP
Fumarate
SAMP
Salvage cytosolic
Cytokinins
Isopentenyl-adenosin-5P
Ade
Ri-1-P
Pi
Ribose
H2O
Ado
ATP
ADP
NMP
NR
PRPP
PPi
Isopentenyl-PP
AMP
Alkaloids
Theobromine
Caffeine
ATP,Gln
AMP,Glu,Pi
IMP
XMP
GMP
NAD
NADH
ADP
ATP
NR
NMP
Inosine
Xanthosine
Guanosine
PPi
PRPP
Nucleoside
Base
Hypoxanthine
Guanine
Xanthine
Uric acid
Allantoin
CO2 + NH3
Urea
Allantoate
Ureidoglycine
NH3
Ureidoglycolate
Urea
Glyoxylate
2 NH3 + CO2
Glyoxylate
Catabolism
Cytosolic/peroxisome

Figure 4. A general schematic outline of plant purine metabolism. The metabolic components shown are: 5-phosphoribosyl-1-pyrophosphate (*PRPP*), glutamine (*Gln*), glutamate (*Glu*), 5-phosphoribosylamine (*PRA*), pyrophosphate (*PPi*), glycine (*Gly*), glycinamide ribonucleotide (*GAR*), 10-formyl tetrahydrofolate (*10F-THF*), formylglycinamide ribonucleotide (*FGAR*), formylglycinamidine ribonucleotide (*FGAM*), 5-aminoimidazole ribonucleotide (*AIR*), 4-carboxy aminoimidazole ribonucleotide (*CAIR*), aspartate (*Asp*), N-succinyl-5-aminoimidazole-4-carboxamide ribonucleotide (*SAICAR*), 5-aminoimidazole-4- carboxamide ribonucleotide (*AICAR*), 5-formaminoimidazole-4-carboxamide ribonucleotide (*FAICAR*), inosine monophosphate (*IMP*), adenylosuccinate (*SAMP*), adenosine monophosphate (*AMP*), xanthosine monophosphate (*XMP*), guanosine monophosphate (*GMP*), adenine (*Ade*), and adenosine (*Ado*). Reprinted from reference 1 with permission from Ann. Rev. Plant Biol. (2006).

two branches. The first branch leads to the formation of adenosine monophosphate (AMP), and the second branch forms guanosine monophosphate (GMP).

Purine catabolism plays an important role in nitrogen metabolism in plants. Animals lack the enzyme uricase and therefore the final product of the purine catabolism is uric acid. Uric acid is excreted as the main source of nitrogen waste. Plants depend on efficient nitrogen utilization and they store nitrogen rather than excreting it (*1*). In plants, the purine nucleotides are oxidatively degraded through uric acid and allantoin to produce CO_2 and NH_3. Both of these are then reabsorbed by the glutamine oxoglutarate aminotransferase (GOGAT) pathway (*1*).

Once AMP is converted to IMP, there are two paths for the catabolism of adenine nucleotides. In the first pathway, which is not shown in Figure 4, IMP is dephosphorylated to inosine by either 5'-nucleotidases or phosphatases. Subsequently, inosine is hydrolyzed to hypoxanthine by inosine/guanine nucleosidase, and then further transformed to xanthine by xanthine dehydrogenase (XDH). In the second pathway, as shown in Figure 4, IMP is converted to XMP by IMPDH which is further metabolized to xanthosine by 5'-nucleotidases. Xanthosine is then converted to xanthine by inosine/guanine nucleosidase (*1*).

Both pathways of adenine nucleotide degradation depend on adenosine monophosphate deaminase (AMPD) because plants lack adenine deaminase and adenosine deaminase (*1*). Although much research supports the lack of adenosine deaminase (ADA) in plants, there is some contradictory evidence. Brawerman and Chargaff first reported the presence of ADA from plants in a commercial sample of malt

diastase (*30*). Later, Fiers *et al.* claimed its presence in extracts from barley rootlets (*31*). Singhabahu *et al.* have also showed the expression of a functional human adenosine deaminase in transgenic tobacco plants (*32*).

Guanosine deaminase on the other hand has been detected in plants. This indicates that guanine nucleotides are degraded through dephosphorylation producing guanosine. Guanosine is either deaminated to xanthosine or transformed to guanine through inosine/guanine nucleosidase, which then gives xanthine (*1*).

The degradation of xanthine leads to the formation of uric acid. Uric acid is then converted to allantoin, which is next converted to allantoate (*1*). In tropical legumes both allantoin and allantoate are important nitrogen storage and transport compounds (*1*). Allantoic acid can be transformed to either ureidoglycine or ureidoglycolate. These products are further metabolized to give the final products of the purine catabolism CO_2, NH_3, and glyoxylate.

The purine *de novo* pathway has a high demand for energy. It hydrolyzes five ATPs to produce a single AMP and seven ATPs to produce a single GMP. On the other hand, the purine salvage pathway conserves energy and hydrolyzes only one ATP (Figure 4). The salvage pathway regenerates plant nucleotide pools. It does so by interconverting nucleosides, nucleotides, and purine bases from plant cell metabolism (*1*). Adenine and guanine can be converted back to their monophosphate forms by adenine phosphoribosyltransferases (APRTase) and hypoxanthine/guanine phosphoribosyltransferases (HGPRTase) using PRPP as a ribose phosphate source. A second route recycles purine bases and uses adenine or inosine guanosine phosphorylase

to synthesize AMP and GMP from adenine and guanine (*1*). Also, converting adenosine, inosine, and guanosine to IMP, XMP, and GMP is catalyzed by either adenosine and inosine/guanine kinases or by nucleoside phosphotransferases.

Nucleoside Hydrolases

Nucleoside hydrolases, also called nucleoside N-ribohydrolases (NHs), are a family of structurally similar metalloproteins with unique central *β*-sheet topology and a group of aspartate residues at the N-terminus of the enzyme (Figure 5) (*4*). NHs catalyze the hydrolysis of the N-glycosidic bond of *β*-ribonucleosides forming a ribose and the corresponding base (Figure 6). NHs are broadly dispersed in nature, and have been discovered in bacteria (*5*, *6*), yeast (*7*), protozoa (*8*, *9*), insects (*10*) and mesozoa (*11*). Genes that include the characteristic NH fingerprint are also found in plants, amphibians and fish (*4*). NHs are also involved in synthesis of plant and bacterial toxins, nucleic acid repair, regulation of calcium ion influx, cytokinin metabolism, and plant purine metabolism (*12*).

NHs play an important role in the purine salvage pathway of parasitic protozoa. Parasitic protozoa such as *leishmania*, *giardia*, and *trypanosome*, rely entirely on the purine salvage pathway for survival, because unlike many other living organisms, they lack the *de novo* synthesis pathway for purines (*4*). Since neither encoding genes nor NH activity has ever been detected in mammals, parasitic protozoan NHs have been studied extensively as a potential target for drug development (*13*).

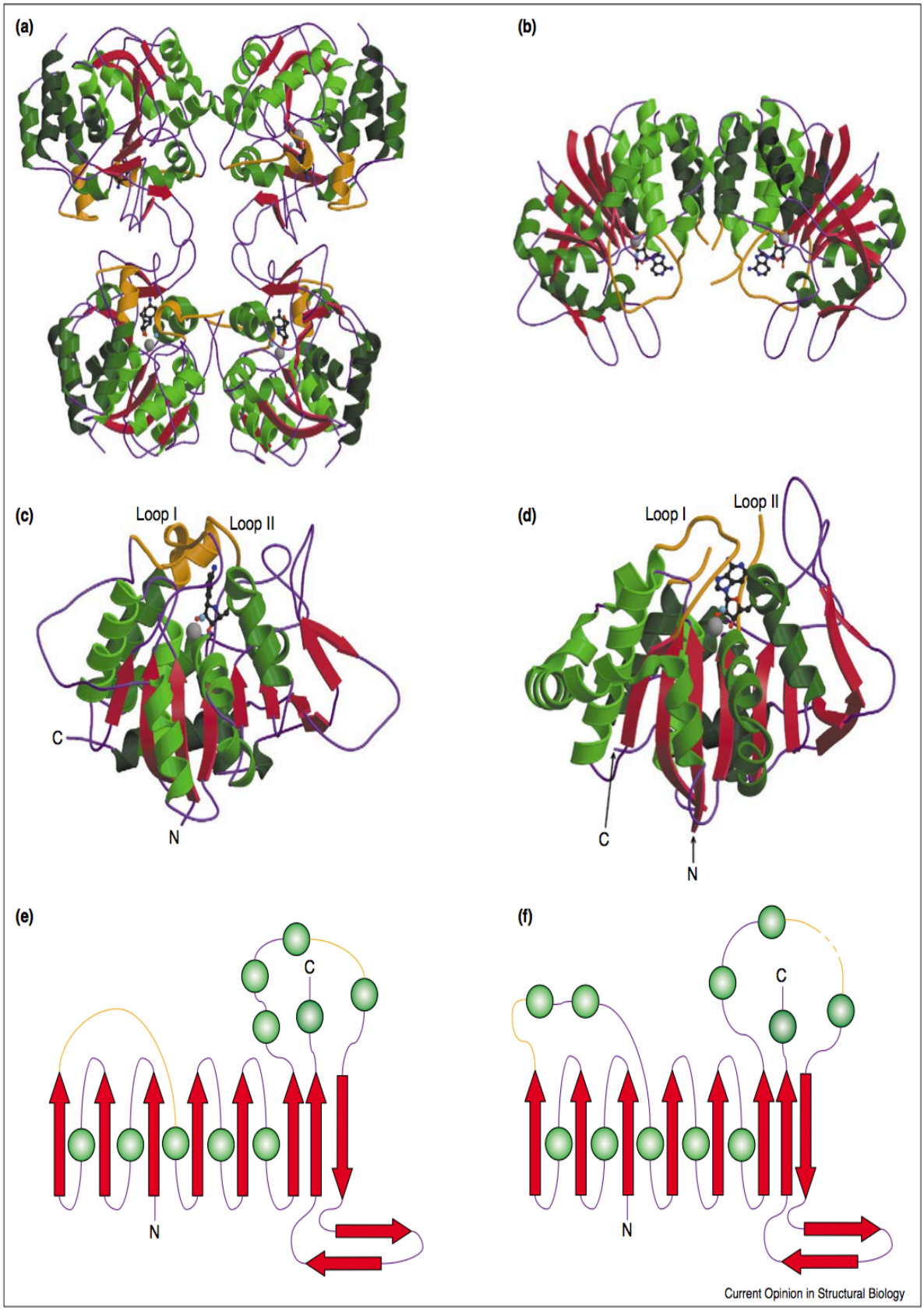
(a)
(b)
(c)
Loop I
Loop II
C
N
(d)
Loop I
Loop II
C
N
(e)
C
N
(f)
C
N
Current Opinion in Structural Biology

Figure 5. Different quaternary nucleoside hydrolase structures are built from a common fold. The topologies, tertiary structures, and quaternary structures of (a,c,e) an IU-NH (*Cf* NH in complex with pAPIR; PDB code 2MAS) and (b,d,f) an IAG-NH (*Tv*NH in complex with 3-deaza-adenosine; PDB code 1HP0) are compared. β Strands are shown in red, and α helices in green. Based on their differences, the order of the helices is indicated by going from light to dark green when going from the N towards the C terminus. Two flexible loops in the area of the active site are shown in yellow. The Ca^{2+} ion and the nucleophilic water molecule are both located in the active site pockets of the enzymes. The Ca^{2+} ion is shown as a grey sphere and the nucleophilic water molecule is shown as a blue sphere. The ligands are represented as ball-and-stick models. Reprinted from reference 4 with permission of Elsevier.

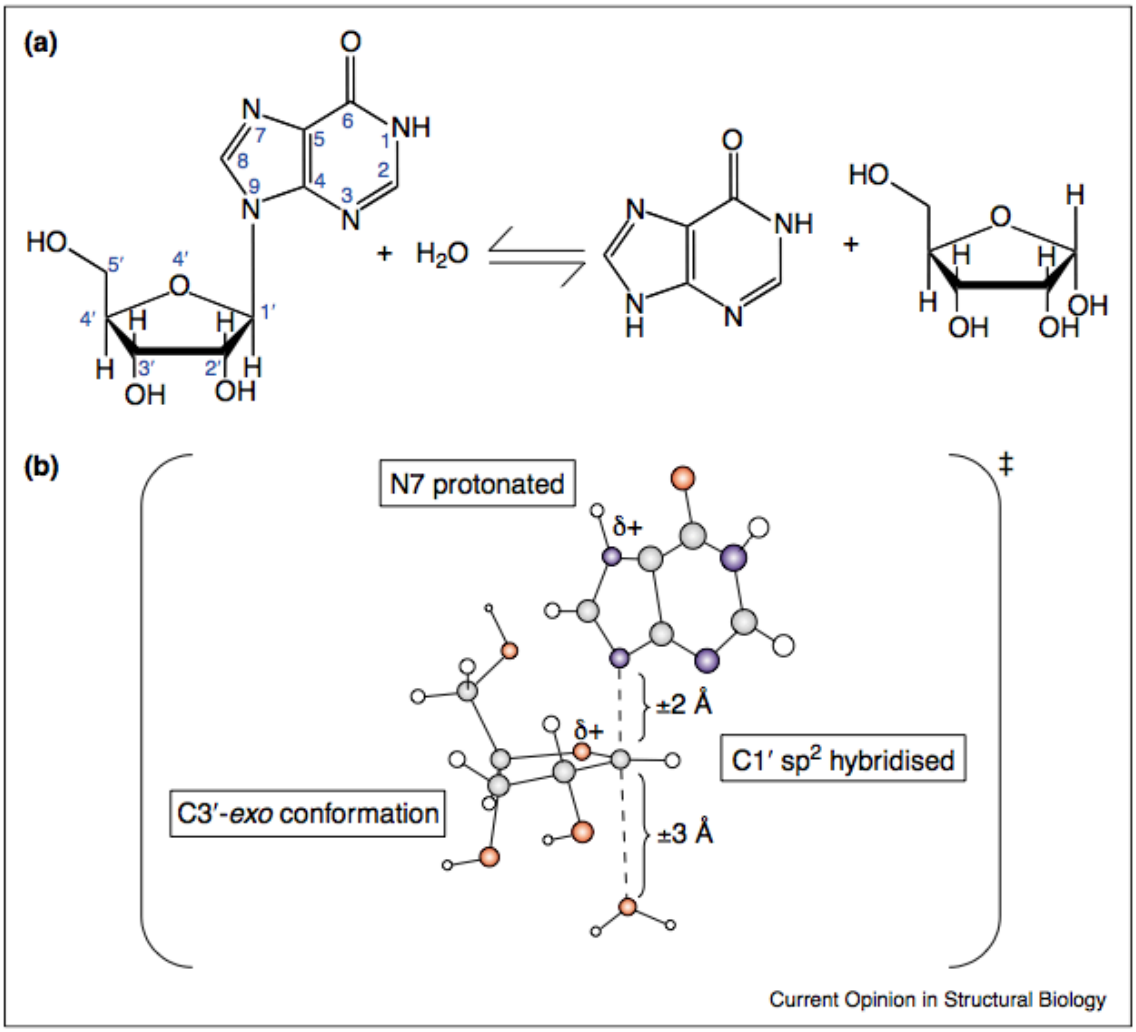

Figure 6. Reaction catalyzed by nucleoside hydrolases. (a) The NH catalyzed the hydrolysis of a ribonucleoside (inosine in this case). The IUPAC-IUB atom numbering order is indicated in blue. (b) The suggested oxocarbenium ion-like transition state for the *Cf* NH catalyzed reaction. Major structural and chemical features of the transition state are also indicated. Reprinted from reference 4 with permission of Elsevier.

The protozoan NHs have been categorized into three subgroups based on their substrate specificity. The first group is the non-specific inosine-uridine preferring nucleoside hydrolases (IU-NHs) (*14*, *15*); the second group is the purine-specific inosine-adenosine-guanosine preferring nucleoside hydrolases (IAG-NHs) (*16*, *17*); and the third group is the 6-oxo-purine-specific inosine-guanosine preferring nucleoside hydrolases (IG-NHs) (*18*). However, recent studies show that this classification is inadequate and that many new NHs do not fit into one of these three groups (*5*, *11*). Also, there is little connection between the level of amino acid identity and the nucleobase specificity, so the existing classification will probably diminish as more NHs are characterized.

The structure of IU-NH from the trypanosome parasite *Crithidia fasciculata* (*Cf* NH) was resolved by Schramm *et al.* using X-ray crystallography to a resolution of 2.5 Å (*19*). The enzyme was in complex with the inhibitor *para*-aminophenyliminoribitol (pAPIR) (*20*). The crystal structure of IU-NH from *Leishmania major* (*Lm*NH) was also solved by the same group. Versees *et al.* reported the crystal structure of the free IAG-specific enzyme, the enzyme complex, and the inhibitor 3-deaza-adenosine from *Trypanosoma vivax* (*Tv*NH) (*16*).

Both IU-NHs from *Crithidia fasciculata* and *Leishmania major* crystallized as similar homotetramers (Figure 5a). The IAG-NH from *Trypanosoma vivax,* on the other hand, is a homodimer in the crystal (Figure 5b). The monomeric subunits of both groups are related in their architecture and topology, and they consist of a single globular domain (Figure 5c,d) (*4*). Interestingly, the subunit of the IAG-NH dimer and the IU-NH tetramers are arranged in different quaternary structures, which involves different

subunit-subunit interfaces. The α/β core of the NH monomer is made of eight-stranded mixed β sheets, where seven of the strands are parallel and one is anti-parallel, and some α helices (Figure 5e,f). The first six β sheet stands resemble a dinucleotide-binding or Rossmann fold (*4*). The location of the active site is at the C-terminal end of this central sheet. There are two flexible loops, loop I and loop II (Figure 5c,d), which are positioned on either side of the active site. Once the transition state inhibitor pAPIR binds to the *Cf* NH enzyme, the loops change their conformation in order to place additional side-chains in the active site to restrict the access of solvent (*20*).

The NHs have one active site per subunit. At the bottom of the active site, there is a Ca^{2+} ion that is tightly bound (Figure 7) (*16*, *20*). The octacoordinated metal is chelated by a network of interactions that involves the side chain oxygens of Asp10, Asp15, Asp261, the carbonyl oxygen of Thr137 (*Tv*NH numbering) and three water molecules. Once the substrate binds, the ribose moiety is secured inside the active site cleft (*4*). After the complex is formed, two Ca^{2+}-bound water molecules are substituted with the 2’-and 3’-hydroxyl groups of the sugar. The last remaining Ca^{2+}-chelated water molecule interacts with aspartate (Asp10). The basis of the strict specificity of the NHs for ribose is found in the complex network of interactions that involves the 2’-, 3’- and 5’ hydroxyls of the sugar and Asp14, Asn173, Glu184, Asn186 and Asp261 (*Tv*NH numbering), and the Ca^{2+} ion (Figure 7).

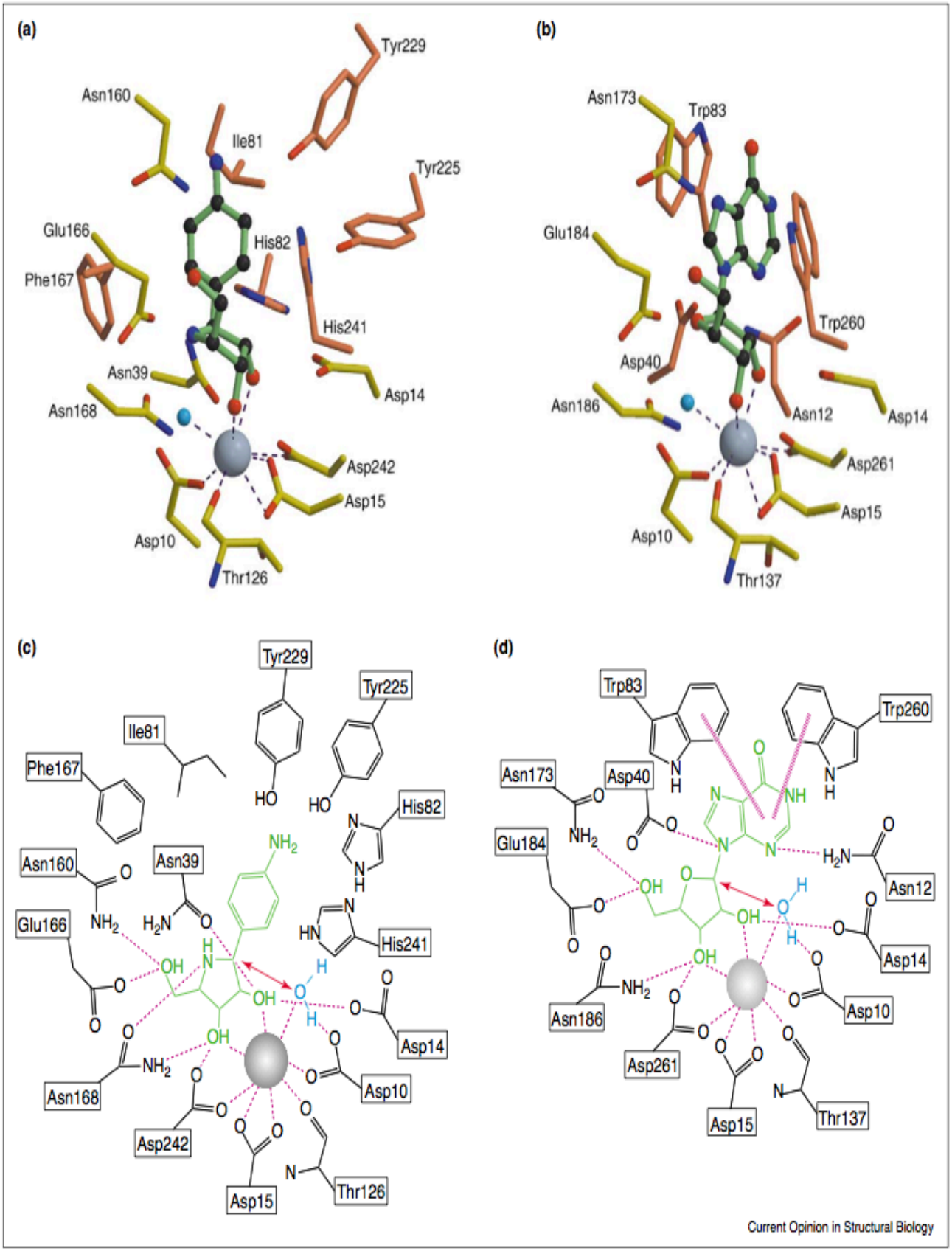
(a)
Tyr229
Asn160
Ile81
Tyr225
Glu166
His82
Phe167
His241
Asn39
Asp14
Asn168
Asp242
Asp15
Asp10
Thr126
(b)
Asn173
Trp83
Glu184
Trp260
Asp40
Asn186
Asn12
Asp14
Asp261
Asp15
Asp10
Thr137
(c)
Tyr229
Tyr225
Ile81
Phe167
His82
Asn160
Asn39
Glu166
His241
Asp14
Asn168
Asp242
Asp10
Asp15
Thr126
(d)
Trp83
Trp260
Asn173
Asp40
Glu184
Asn12
Asp14
Asp10
Asn186
Asp261
Asp15
Thr137
Current Opinion in Structural Biology

Figure 7. Comparison between the active sites of (a,c), an IU-NH (*Cf* NH in complex with pAPIR) and (b,d) an IAG-NH (*Tv*NH in complex with inosine). The enzyme bound ligands are indicated in green. The Ca^{2+} ion is shown as a grey sphere and the nucleophilic water molecule is shown as a blue sphere. In (a,b), the active site residues that have strong interactions with the Ca^{2+} ion and the ribose moiety are shown in yellow, while the residues of the nucleobase-binding pocket are shown in light brown. The intermolecular interactions are represented schematically in (c,d). Other possible interactions are indicated by the dotted lines. The arrows indicate the nucleophile and the electrophilic center of the substitution reaction. The nucleobase in the *Tv*NH–inosine complex is arranged between the side chains of Trp83 and Trp260 (d). The poor analogy of the p-aminophenyl group with real nucleobases does not allow a direct analysis of catalytic interactions in the nucleobase-binding pocket of *Cf* NH (c). Reprinted from reference 4 with permission of Elsevier.

Adenosine Nucleosidase

Adenosine nucleosidase is an important enzyme in the purine salvage pathway in plants. Adenosine nucleosidase catalyses the irreversible hydrolysis of adenosine (Ado) to adenine (Ade) and ribose (Figure 8). Adenosine nucleosidase is believed to control the levels of cytokinins, which affects the growth of plants (*23*). The ability of plants to recycle adenine can be measured by the amount of adenosine nucleosidase. One study revealed that fruitful apple and cherry trees showed adenosine nucleosidase levels three times higher than the wild types (*12*).

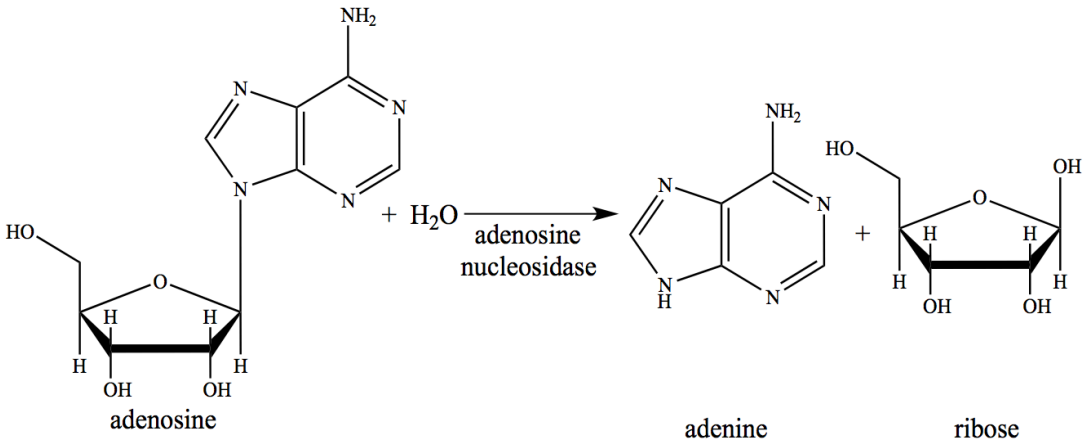

Figure 8. Hydrolysis of adenosine to adenine and ribose by adenosine nucleosidase.

Adenosine nucleosidase was first purified by Miller and Evans from soybean leaves (*21*). Since then, it has been purified from many other plant sources such as spinach beet leaves (*22*), barley leaves (*23*), tea leaves (*24*), wheat germ (*25*), Jerusalem

artichoke shoots (*26*), tomato roots and leaves (*27*), yellow lupin seeds (*28*), and Alaska pea seeds (*35*).

Adenosine nucleosidase from leaves of spinach beet (*Beta vulgaris L.*) was partially purified by Poulton and Butt (*22*). The optimum pH was 4.5 and the K_m for adenosine was 11 μM. The enzyme was specific for adenosine and did not utilize other nucleosides as substrates. Yet, there was comparable activity with adenosine N-oxide. Oxidizing adenosine produces adenosine N-oxide, which has a nitrogen monoxide bond.

Guranowski *et al.* purified adenosine nucleosidase from barley leaves (*23*). Using gel filtration chromatography, the molecular weight was determined to be 66,000 daltons. SDS-PAGE showed that the enzyme is a dimer and has a subunit molecular weight of 33,000 daltons. The optimum pH was 4.7 for citrate and 5.4 for ethanesulphonic acid buffers. Depending on the temperature and the buffer system, the K_m for adenosine ranged from 0.8 to 2.3 μM. Adenosine N_1-oxide, deoxyadenosine and purine riboside were substrates for the enzyme, while adenine and cytokinins inhibit the enzyme.

Imagawa *et al.* were able to purify three types of adenosine nucleosidase called adenosine nucleosidase I, II, and III from tea leaves (*24*). The molecular weight of all three types was approximately 68,000 daltons. The optimum pHs for types I and III were 4.0, and 4.5 for type II. The substrate specificity was similar in all three adenosine nucleosidases. Adenosine and 2'-deoxyadenosine were the only naturally occurring nucleosides that were hydrolyzed by the three enzymes. The hydrolysis rate was three to four times higher for 2'-deoxyadenosine compared to adenosine.

Chen and Kristopeit partially purified adenosine nucleosidase from wheat germ cells (*25*). The molecular weight was determined to be 59,000 ± 3000 daltons. The optimum pH was 4.7. The K_m was 2.3 μM for cytokinin nucleoside and 1.43 μM for adenosine.

Le Floch *et al.* purified purine nucleosidase from Jerusalem artichoke shoots (*26*). The extract exhibited adenosine and inosine-guanosine nucleosidase activities. The result suggests that two different enzymes with some similar properties exist. Some of the similar properties include high stability, optimal pH from 5 to 7 and high affinity for substrates. The K_m was 17 μM for adenosine, 8.5 μM for guanosine, and 2.5 μM for inosine. The two enzymes were distinguished by their substrate specificity. The addition of adenosine had no effect on the rate when either inosine or guanosine acted as a substrate. However, addition of 6-mercaptopurine riboside strongly inhibited the hydrolysis of inosine and guanosine, but had no effect on the hydrolysis rate of adenosine.

Burch and Stuchbury partially purified adenosine nucleosidase from tomato roots and leaves (*27*). Using DEAE-cellulose columns, two different forms of adenosine nucleosidase, R1 and R2, were found in the tomato roots. Furthermore, a single type of adenosine nucleosidase, Lf, was found in the tomato leaves. The optimum pH was 5.0 for R1, and 6.0 for R2 and Lf. The K_m values for these enzymes using adenosine as the substrate were 25 μM for R1, 9 μM for R2, and 6 μM for Lf. A molecular weight of 68,000 daltons was estimated for R2 adenosine nucleosidase, which is the major enzyme component of the root. R2 and Lf adenosine nucleosidase are similar to each other while

they differ from the R1 enzyme. For all three enzymes, cytokinin ribosides acted as a competitive inhibitor.

Abusamhadneh *et al.* purified adenosine nucleosidase from yellow lupin seeds (*28*). A yield of 2.3 % with a 74-fold purification was accomplished. A molecular weight of 177,000 daltons, an optimum pH of 7.5, and a K_m of 4.7 μM for adenosine were determined. The enzyme showed activity with adenosine, 2'-deoxyadenosine, guanosine, cytidine, inosine and thymidine, with the highest activity for adenosine.

Altawil purified adenosine nucleosidase from Alaska pea seeds (*35*). Some characterization of the enzyme was done in this work, and the subunit molecular weight was determined by SDS-PAGE to be 36,000 daltons.

Cytokinins, which are mostly made of adenine or adenosine derivatives, are plant hormones that have numerous physiological effects on plants. When these physiological effects are used to their greatest potential, the result is highly beneficial to agriculture. Several studies have shown that exogenous cytokinins can increase crop yield, delay senescence, improve flowering, and control bug outgrowth (*12*). Adenosine nucleosidase and some cytokinin metabolizing enzymes may be involved in either the regulation of the level of cytokinin that is available to the plant cells or the regulation of cytokinin metabolic pathway (*12*). In some plants however, cytokinins are not good substrates for adenosine nucleosidase. As a result, adenosine nucleosidase is more likely to indirectly regulate the level of cytokinins by controlling the levels of adenine, which in turn can be used to form cytokinins (*12*).

CHAPTER II

MATERIALS AND METHODS

Equipment and Instrumentation

An Allegra 64R centrifuge from Beckman Coulter and Sorvall Evolution RC centrifuge were used to centrifuge and concentrate the samples depending on their volume. Mono Q and Hydroxyapatite chromatography were carried out on an AKTA Fast Protein Liquid Chromatography (FPLC) system from GE Healthcare. High performance liquid chromatography (HPLC) was performed on a Dionex Ultimate 3000 HPLC system. Mass spectrometry was carried on a Thermo Scientific MSQ Plus mass spectrometer. UV-Vis spectroscopy was carried out on a Hitachi U-2900 spectrophotometer.

Materials and Reagents

Alaska (Wilt Resistant) pea seeds were obtained from Ferry-Morse Seed Company. Adenosine, uridine, inosine, cytidine, thymidine, 2′-deoxyadenosine, cordycepin, tubercidin, 5-methyluridine, and benzamidine were obtained from Sigma. Dithiothreitol, gel filtration standard, Bio-Rad protein assay standard II, and Precision Plus Protein™ Unstained Standards were obtained from Bio-Rad. Ammonium sulfate and Lonza Precast 15 % gels were obtained from Fisher Scientific. Potassium phosphate and neocuproine hydrochloride monohydrate were obtained from Acros. Ammonium

phosphate monobasic was obtained from J.T. Baker Chemical Co. All other chemicals were reagent grade. The water used to prepare solutions was deionized on an ELGA Purelab Ultra and was at least 18 MΩ.

Preparation of Enzyme Extract

Alaska pea seeds (50.3 g) were thoroughly washed with deionized water three times. The seeds were placed on a dampened brown paper towel, and allowed to germinate for five days at room temperature. The seeds were then homogenized in a blender in 265 mL of 10 mM Tris buffer, pH 7.2. About 10 mg of benzamidine, dithiothreitol, and deoxyribonuclease from bovine pancreas were added to the homogenization solution, and the blender ran for two minutes. This step of the procedure was carried out in the cold room at 4 °C. The resulting slurry was filtered through a double layer of cheesecloth. Next, the homogenate was centrifuged in the Allegra 64R centrifuge at 20,000 *xg* for 15 minutes at 4 °C to remove large particles, and the supernatant was saved.

Enzyme Purification

Ammonium Sulfate Precipitation

A total of 40 g of solid ammonium sulfate was gradually added to the supernatant (225 mL) to bring the solution to 30 % saturation (*33*). The sample was stirred slowly

until the ammonium sulfate was dissolved. The beaker was covered in foil and was left over night in the cold room at 4 °C.

The sample was centrifuged in the Allegra 64R centrifuge for 30 minutes at 20,000 *xg* at 4 °C. The 30% supernatant was saved (240 mL) and 55 g of solid ammonium sulfate was added to increase the saturation to 60%. The solution was again left over night in the cold room at 4 °C. The sample was centrifuged for 30 minutes at 25,000 *xg* at 4 °C. The pellet was recovered and the supernatant was discarded. In order to resuspend the precipitate, 15 mL of a 10 mM Tris buffer pH 7.2 was added to each centrifuge bottle. The bottles were placed in a laboratory rocker in the cold room until the pellet was resuspended. Once the pellet was resuspended, it was dialyzed against 1 L of 10 mM Tris buffer pH 7.2 overnight in the cold room at 4 °C.

Ion Exchange Chromatography

To prevent clogging the FPLC, the sample was centrifuged at 8,000 *xg* at 4 °C for 30 minutes. Using a Centricon concentrator tube, the sample was concentrated to a total volume of 15 mL. The first 5 mL of the sample was loaded on a Mono Q FPLC column.

The column used was HiPrep 16/10 Mono Q Fast Flow (HiPrep 16/10 Q FF). The flow rate was 5 mL/min. After injecting the sample onto the column, the column was washed with five column volumes. The fraction size was 10 mL. Two different buffers were used. The low salt buffer, buffer A, was a 10 mM Tris buffer pH 7.2, and the high salt buffer, buffer B, was a 10mM Tris + 1M NaCl pH 7.2 buffer. A linear gradient from

zero percent buffer B to one hundred percent buffer B was run over 20 column volumes. The column volume was 20.1 mL, so the linear gradient total volume was 402 mL going from zero percent to one hundred percent buffer B. The effluent was monitored at 280 nm. Two additional samples were chromatographed on the Mono Q column under the same conditions. Samples from each FPLC run were stored in the cold room until all three FPLC runs were finished. All the fractions were assayed for activity by reducing sugar assay (*34*).

Measurement of Enzyme Activity by Reducing Sugar Assay

First, a 1mM adenosine reaction mixture was made by the following procedure. The required amount of adenosine to make 100 mL of a 1 mM solution was calculated by the following method:

$$1\ mM\ of\ Adenosine \rightarrow \frac{1\ mmol}{L} * \frac{267.4\ mg}{mmol} * 0.1L = 26.7\ mg$$

Adenosine was measured (26.72 ± 0.2 mg) and 5 mL of 1M Tris buffer pH 7.2 was added. Water (95 mL) was then added to the mixture and the solution stirred until the adenosine dissolved. The pH was adjusted to 7.2 using either HCl or NaOH. One mL from the adenosine reaction mixture was added to separate test tubes for each fraction from the column. The reaction was started by adding 100 µL of solution from each fraction from the Mono Q column to each test tube. In the control, 100 µL of water was added instead of the enzyme solution. The test tubes were then placed in a 32 °C water bath for 3 hours. The reaction was stopped by adding 300 µL of the copper reagent and

then vortexing the test tubes. The copper reagent was 4% Na_2CO_3, 1.6% glycine, and 0.045% $CuSO_4 \bullet 5H_2O$ dissolved in 400 mL water. Next, 300 µL of neocuproine reagent was added and the test tubes were placed in boiling water (90-100 °C) for 7 minutes. The neocuproine reagent consists of 0.12% neocuproine (0.48 g) dissolved in 400 mL water, pH adjusted to 3.0 using HCl. The final step was to measure the absorbances at 450 nm after the test tubes cooled. The amount of ribose was determined by comparing the results to a standard curve (Figure 9).

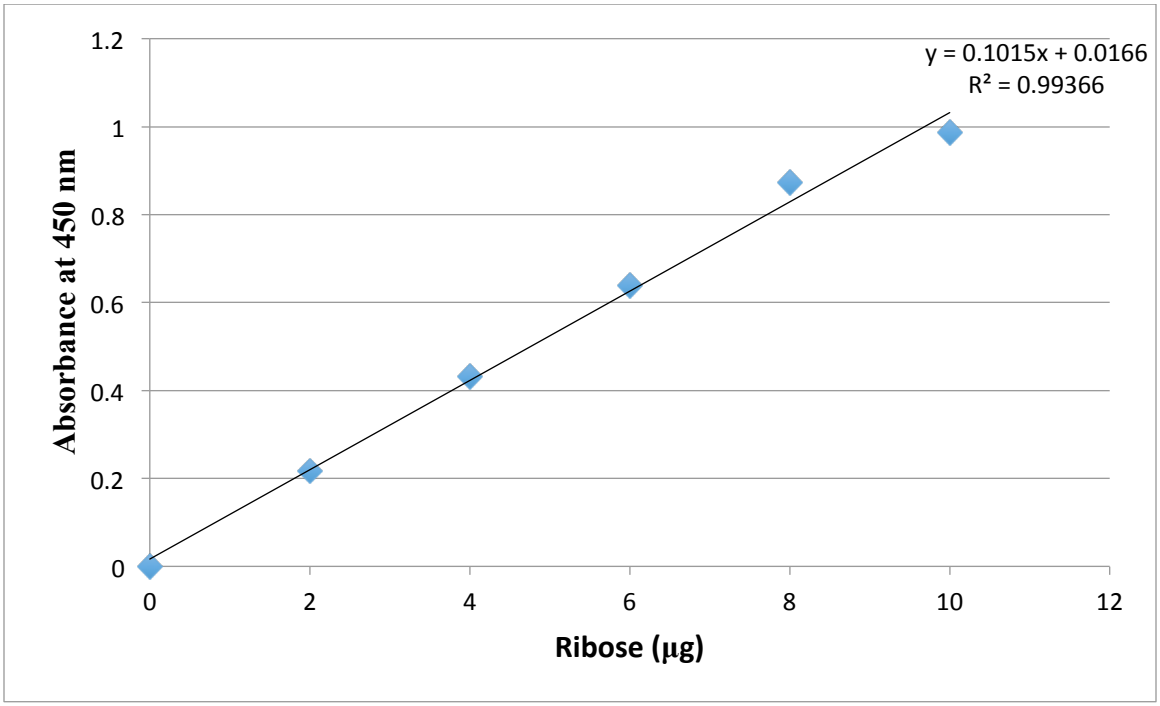

Figure 9. Reducing sugar assay calibration curve. The activity of the enzyme was determined by the appearance of reducing sugar.

Fractions with the highest activity were pooled and concentrated. Fractions numbers 12 – 15 from all three runs (total of twelve fractions) were pooled and labeled as pool #1. Fractions numbers 16 –19 from all three runs (total of twelve fractions) were pooled and labeled as pool #2. The fractions were pooled in this manner because the absorbance readings were similar in all three runs. Both of the pooled fractions, pool #1 and pool #2, were concentrated down to 5 mL using the Amicon ultrafiltration concentrator in the cold room instead of the centricon concentrator tubes due to the large volume of the samples.

Hydroxyapatite Chromatography

Both samples (pool #1 and pool #2) were dialyzed against 1 L of 10 mM phosphate buffer pH 7.2 and placed in the cold room. This was repeated twice over two days replacing the buffer two times. After the dialysis, there were approximately 6 mL of each sample. The samples were then loaded on the hydroxyapatite column one at a time.

The column used was BioRad-CHT1-Hydroxyapatite. The flow rate was 1 mL/min. After injecting the sample onto the column, the column was washed with six column volumes of Buffer A. The fraction size was 5 mL. The low salt buffer, Buffer A, was 10 mM potassium phosphate buffer pH 6.8, and the high salt buffer, Buffer B, was 400 mM potassium phosphate buffer pH 6.8. A linear gradient was run from zero percent Buffer B to one hundred percent Buffer B over 20 column volumes. The column volume was 5 mL, so the linear gradient total volume was 100 mL. The effluent from the column

was monitored at 280 nm. After the fractions were collected from the hydroxyapatite column, 60 fractions in total, the reducing sugar assay was done using the method described above. The fractions with high absorbances were pooled. Fraction numbers 14 – 17 from both runs (8 fraction in total) were polled and named pool #1. Fraction numbers 20 – 23 from both runs (8 fraction in total) were pooled and named pool #2. Both samples, pool #1 and pool #2 from the hydroxyapatite column, were then concentrated down to 5 mL.

Determination of Molecular Weight

SDS-PAGE

A sodium dodecyl sulfate polyacrylamide gel electrophoresis (SDS-PAGE) was run on pool #1 and pool #2 from the hydroxyapatite column using a 15 % Lonza Precast gel to estimate their subunit molecular weight and determine the purity of the sample. The samples were loaded onto the gel along with the Precision Plus Protein™ Unstained Marker. The gel ran for 50 minutes with a voltage of 158 V and a current of 13 mA. After completion, the gel was placed into a container and covered with Gelcode Blue Safe protein stain and left overnight. A calibration curve was constructed using the Precision Plus Protein™ Unstained molecular weight marker. The molecular weight of the samples was determined by comparing them to the calibration curve. The purity of the sample was determined based on a visual inspection of the intensity of the coomassie blue band, and it was determined that the enzyme was 95% pure.

Mass Spectrometry

In order to acquire the most accurate molecular weight measurement, the samples were analyzed by mass spectrometry. The column used was a Phenomenex Jupiter C18 300A 5um, 50 x 4.6 mm. The mobile phase was 80% A (0.05 % formic acid in water), and 20% B (0.05 % formic acid in acetonitrile). Flow rate was 0.6 mL/min. The ionization mode was ES-API, and the polarity was positive. Fragmentation voltage was 90 V, and the gas drying temperature was 350 °C. The m/z range was 500-2000 daltons.

Determination of Protein Concentration

Bio-Rad Assay

One method of determining the protein concentration was by the Bio-Rad dye assay. The assay mixture contained water and enzyme solution totaling 800 µL, to which 200 µL of dye was added. The absorbance of the assay mixtures were then measured at 595 nm. The protein concentrations of each purification step and the purified enzyme was determined by comparing the results to a calibration curve that was constructed using the Bio-Rad protein assay standard bovine serum albumin (Figure 10).

UV-Vis Assay

The protein concentration of both samples, pool #1 and pool #2, from the hydroxyapatite chromatograph were determined by measuring their absorbances at 280

nm. The protein concentration in µg/mL was determined using the equivalence of absorbance at 280 nm = concentration in mg/mL.

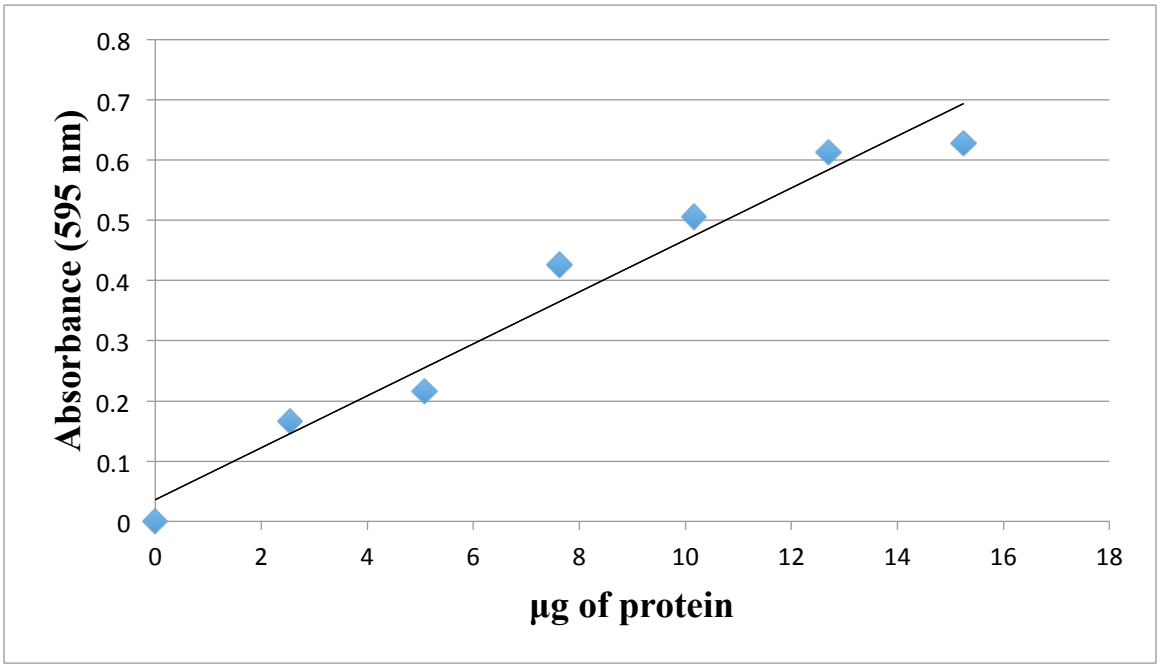

Figure 10. Protein concentrations calibration curve determined at 595 nm using Bio-Rad protein assay standard bovine serum albumin.

Measurement of Enzyme Activity

Throughout the purification process, enzyme activity was measured by a reducing sugar assay (as described above), or by measuring the relative amounts of nucleoside and base, as determined by HPLC, in a given amount of time.

HPLC Analysis

The activity was measured in 1 mL of 1 mM adenosine in 10 mM Tris pH 7.2. The reaction was initiated by the addition of 50 μL of enzyme. When testing the activity of the sample from the hydroxyapatite column, 100 μL of the enzyme was added instead of 50 μL. In the control, water was added instead of the enzyme solution. The reaction mixture was incubated at room temperature and aliquots removed at time intervals to determine the relative amount of nucleoside and base. The HPLC column used to separate the nucleoside and base was a Hyperclone 5u ODS (C18) reverse phase (150 x 4.6 mm) column. The temperature of the column oven was 30.0 °C. The mobile phases were 2 % methanol and 98 % 10 mM ammonium phosphate buffer pH 5.4. The reaction was monitored at 254 nm. The flow rate was 0.8 mL/min. The retention time of adenosine was 20.7 minutes and adenine was 6.9 minutes. The amount of adenosine and adenine present were calculated based on their respective peak areas. Activity was calculated by the disappearance of adenosine.

Steady State Kinetic Analysis

The activity of the enzyme was measured using adenosine as the substrate. The progress of the reaction was monitored by HPLC as described above. An aliquot of the enzyme solution (25 μL) was added to reaction mixtures containing variable concentrations of adenosine in 50 mM Tris pH 7.2. In the control, 25 μL of water was

added instead of the enzyme solution. The concentrations of adenosine used were approximately 50, 100, 250, 500, 850, 1000, and 1500 μM.

Substrate Specificity

Several substrates were tested for activity against the enzyme purified. The substrates tested are listed in Table 1. The reaction mixture consisted of 1 mM nucleoside in 10 mM Tris pH 7.2. The reaction was started by the addition of 25 μL of enzyme. In the control, 25 μL of water was added instead of the enzyme solution. The reaction was incubated overnight and the relative amount of nucleoside and base were determined by the areas of the respective nucleoside and base.

Table 1. Nucleosides used as substrates to test the activity of the enzyme.

Nucleosides Used as Substrate	
Adenosine	2'-Deoxyadenosine
Guanosine	3'-Deoxyadenosine (cordycepin)
Inosine	5'-Deoxyadenosine
Uridine	7-Deazaadenosine (tubercidin)
Cytidine	5-Methyluridine
Thymidine	Uracil-1-β-D-arabino-Furanoside
	Purine Riboside

CHAPTER III

RESULTS AND DISCUSSION

Adenosine nucleosidase catalyses the irreversible hydrolysis of adenosine to adenine and ribose. Adenosine nucleosidase is an important enzyme in purine metabolism in plants. The reason this enzyme was studied was because it was hypothesized that it might be important in affecting and controlling the cytokinins. Cytokinins are plant hormones and they are all derivatives of adenosine, and the enzyme that was studied is called adenosine nucleosidase. Even though the physiological role of adenosine nucleosidase is not yet fully understood, it may be important in controlling the cytokinins indirectly. Since cytokinins themselves have never been found to be substrates, adenosine nucleosidase might control cytokinins by controlling the availability of adenosine to make the cytokinins, which in turn controls a whole series of plant processes. For example, cytokinins are involved primarily in cell growth and differentiation, but also affect apical dominance, axillary bud growth, and leaf formation and senescence. Also, cytokinins are an essential ingredient in medium for growing plant cells in culture, and without them in the medium, plant cells would not divide by mitosis. A better understanding of adenosine nucleosidase might lead to a better understanding of cytokinins metabolism. This enzyme has been isolated from many different plants, and the results showed differences in their physical characteristics, substrate specificity, optimum pH, and K_m values.

Purification of Adenosine Nucleosidase

Adenosine nucleosidase was purified from Alaska pea seeds. Five days after germination, 50 g of seeds were homogenized. The sample was filtered through cheesecloth and then centrifuged to remove large particles. Using 1 mM adenosine as a substrate, the activity of the initial extract was assayed by HPLC. The chromatogram shows multiple peaks, which indicates the presence of several enzymes (Figure 11). Based on the nucleosides and bases present, the enzymes present in the sample are adenosine nucleosidase, adenosine deaminase, and inosine nucleosidase. The specific activity of the initial extract was 7.3 x10^{-3} µmol/min/mg based on the loss of adenosine.

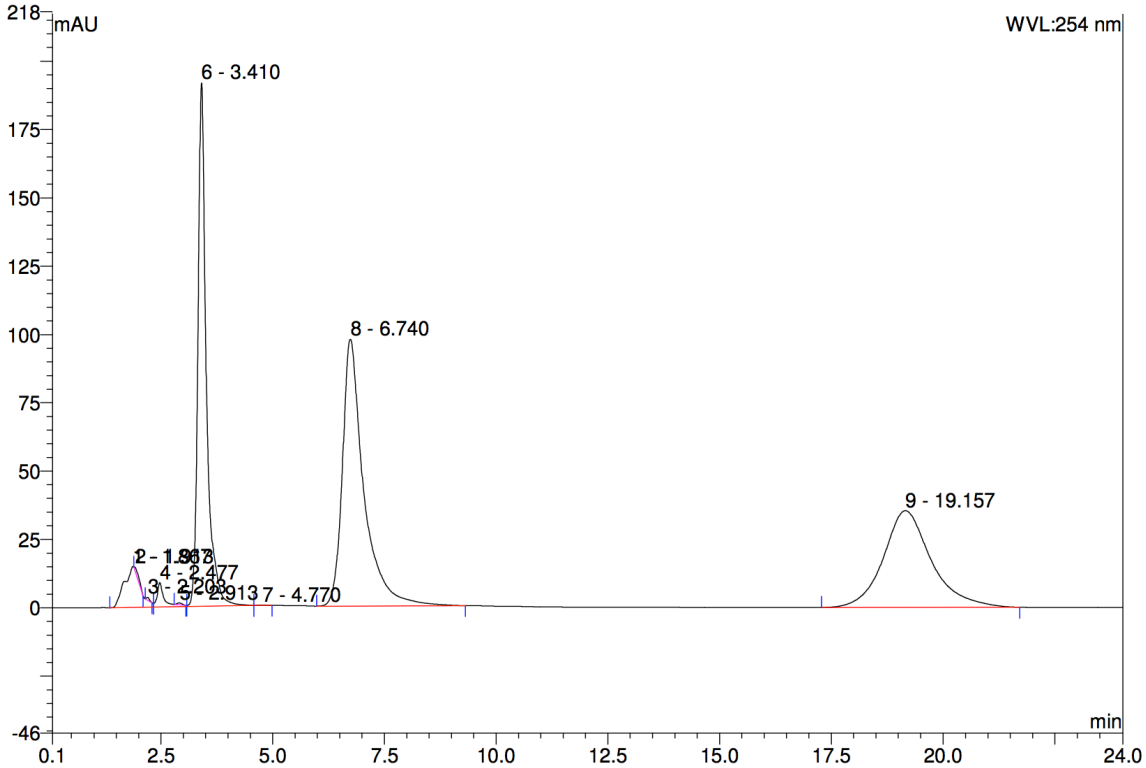

Figure 11. HPLC analysis of activity of initial extract. The reaction mixture consisted of 1 mL of 1 mM adenosine in 10 mM Tris pH 7.2. + 50 µL of initial extract. After 6.5

hours, the chromatogram shows adenosine (19.15 min), adenine (6.74 min), and hypoxanthine (3.41 min).

After centrifuging the initial extract sample to remove debris, the next step was an ammonium sulfate precipitation. After adding the solid ammonium sulfate to the initial extract, the saturation level was 30%. It is important to allow time for the ammonium sulfate to dissolve before adding more to the sample. The solution was stored in the cold room overnight at 4°C. After centrifuging the sample and removing the precipitated proteins, additional solid ammonium sulfate was added to the 30% supernatant in order to reach 60% saturation. The solution was stored in the cold room overnight at 4°C. After centrifuging the sample, the pellet was saved and was resuspended in 30 mL of a 10 mM Tris buffer pH 7.2.

Both samples, the 30% supernatant and the 60% resuspended pellet, were assayed for activity by HPLC. The chromatogram of both 30% and 60% saturation levels showed multiple peaks, again indicating the presence of several enzymes (Figure 12a, 12b). The results in the reaction profile show the presence of two nucleoside metabolizing enzymes, adenosine deaminase, and adenosine nucleosidase. Adenosine deaminase converts adenosine to inosine, and adenosine nucleosidase converts adenosine to adenine and inosine to hypoxanthine. The 30% saturation gave a specific activity of 8.1 $x10^{-3}$ μmol/min/mg. Once 60% saturation was reached, the specific activity was 5.3 $x10^{-3}$ μmol/min/mg.

After dialyzing and concentrating the resuspended 60% pellet solution, the sample was loaded onto a Mono Q ion-exchange chromatography column. Ion-exchange chromatography separates molecules based on differences in charge. The separations of the molecules are based on the reversible interaction between the charged chromatography medium and the oppositely charged proteins in the sample. Based on the type of the ligand used, ion-exchange chromatography can be classified into two types.

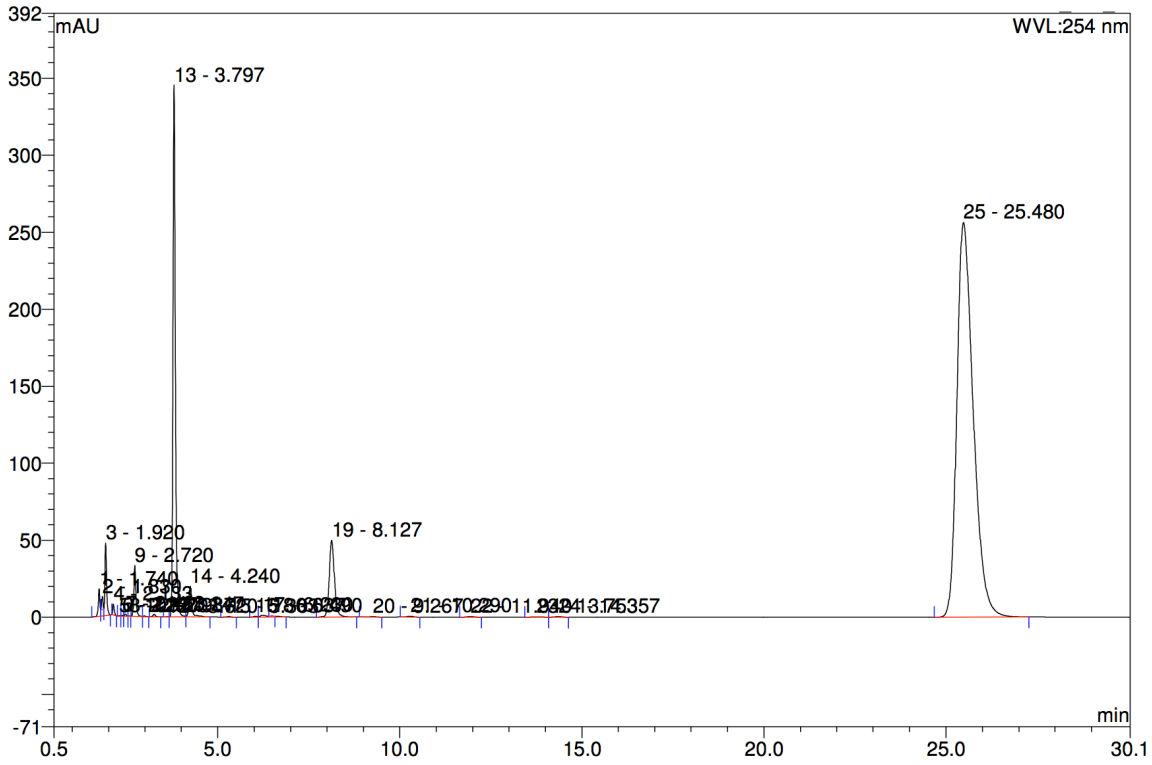

Figure 12a. HPLC analysis of activity of 30% saturation sample. The reaction mixture consisted of 1 mL of 1 mM adenosine in 10 mM Tris pH 7.2. + 50 µL of 30% saturation sample. After 7 hours, the chromatogram shows adenosine (25.48 min), adenine (8.12 min), and hypoxanthine (3.79 min).

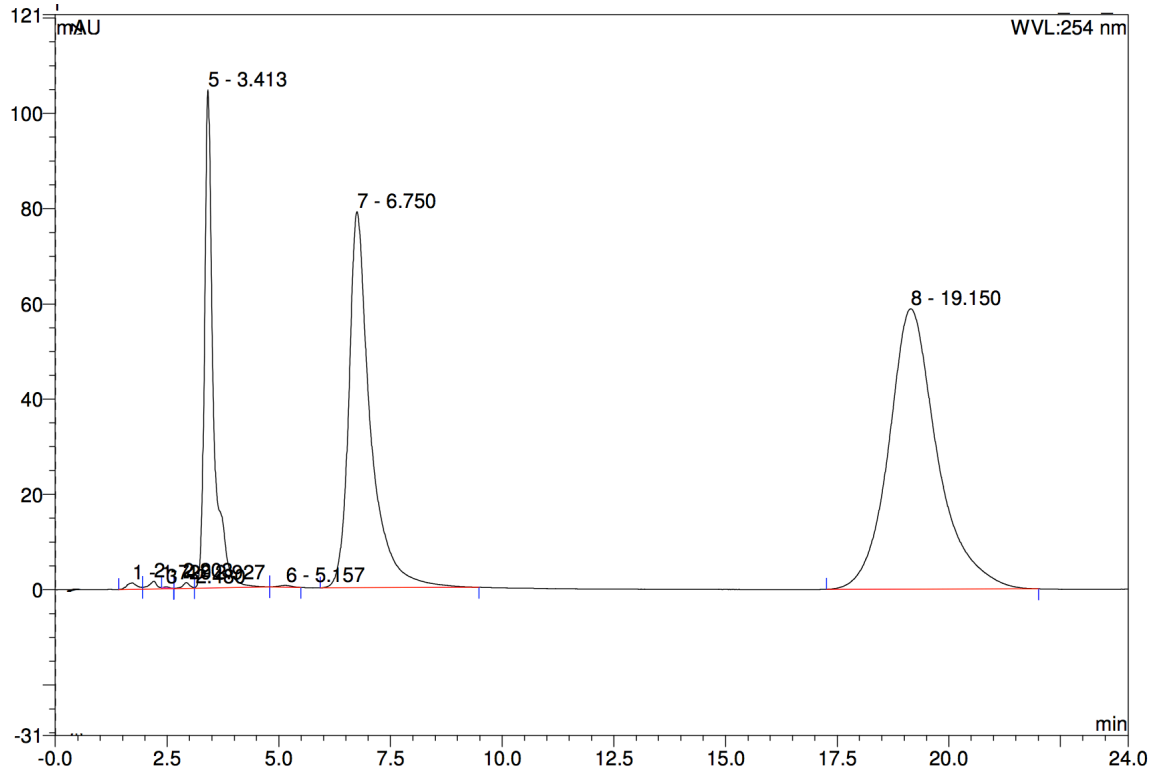

Figure 12b. HPLC analysis of activity of 60% saturation pellet. The reaction mixture consisted of 1 mL of 1 mM adenosine in 10 mM Tris pH 7.2. + 50 µL of 60% saturation pellet. After 7 hours, the chromatogram shows adenosine (19.15 min), adenine (6.75 min), and hypoxanthine (3.41 min).

The first type is anion exchange chromatography, in which the positively charged cation in the stationary phase binds to the negatively charged proteins in the sample. The second type is cation exchange chromatography, in which the negatively charged anion in the stationary phase binds to the positively charged proteins in the sample (*35*). Typically, the conditions are selected so that once the sample is loaded onto the column, the molecule of interest binds to the medium (*36*). Conditions are then altered so that the bound molecules are eluted distinctively. Elution is often performed by a linear gradient

or by a step increase in ionic strength, most commonly using NaCl (*36*). The Mono Q column that was used was a strong anion exchanger packed with Q Sepharose Fast Flow. It gave fast, reliable, and reproducible results (*37*).

The first 5 mL of the sample (15 mL total) was loaded into the column, and then two additional samples were chromatographed. A linear gradient was run from 0 to 1M NaCl in 10 mM Tris pH 7.2. Looking at the elution profile of all three samples, a total of six peaks were detected by UV (Figures 13, 15, 17). The first three peaks were eluted in the wash, while the other three were eluted during the linear gradient. Since the Mono Q column is positively charged and the enzyme bonded to its resin and came out in the gradient, this indicated that the enzyme has an overall negative charge. The chromatograms also show the accuracy of the instrument. The results were reproducible for all three runs.

A reducing sugar assay was done on the fractions collected and the fractions that produced the most ribose were pooled and concentrated (Figures14, 16, 18). Fraction numbers 12 – 15 and 16 –19 from all three runs were pooled and labeled as pool #1 and pool #2 respectively. The activity of the pooled samples were tested by HPLC analysis using adenosine as a substrate (Figures 19 and 20). This step gave 4 fold-purification. The overall purification after this step was 3-fold with 7.9 percent recovery. The specific activity increased to 2.1×10^{-2} μmol/min/mg.

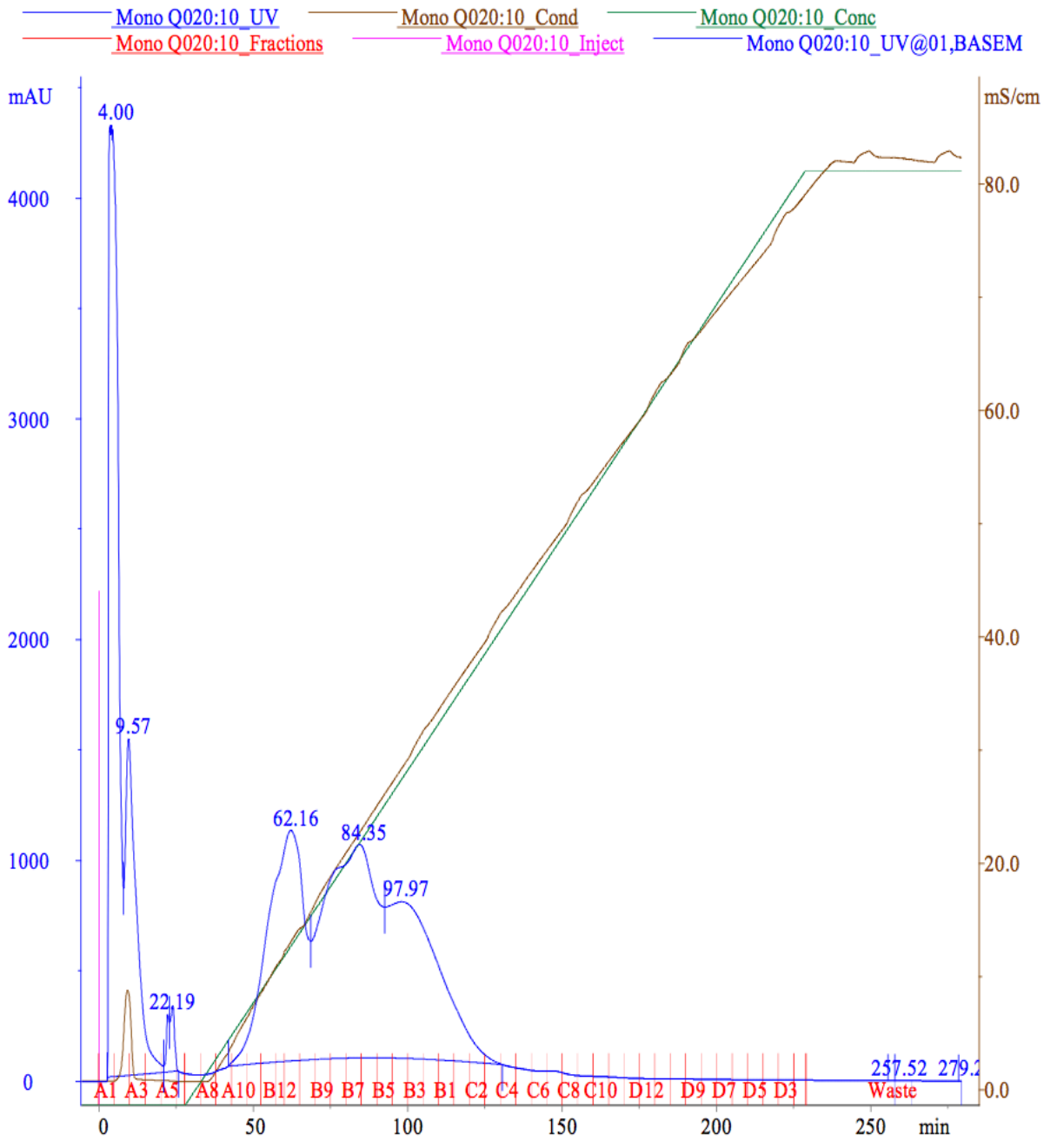

Figure 13. Elution profile (first 5 mL out of 15 mL of total sample) from Mono Q ion exchange chromatography column. The fraction size was 10 mL. Flow rate was 5 mL/min. Two different buffers were used. The low salt buffer, buffer A, was 10 mM Tris buffer pH 7.2, and the high salt buffer, buffer B, was 10 mM Tris + 1M NaCl pH 7.2 buffer. A linear gradient from 0% buffer B to 100% buffer B was run over 20-column volume. The gradient started at 50 mL.

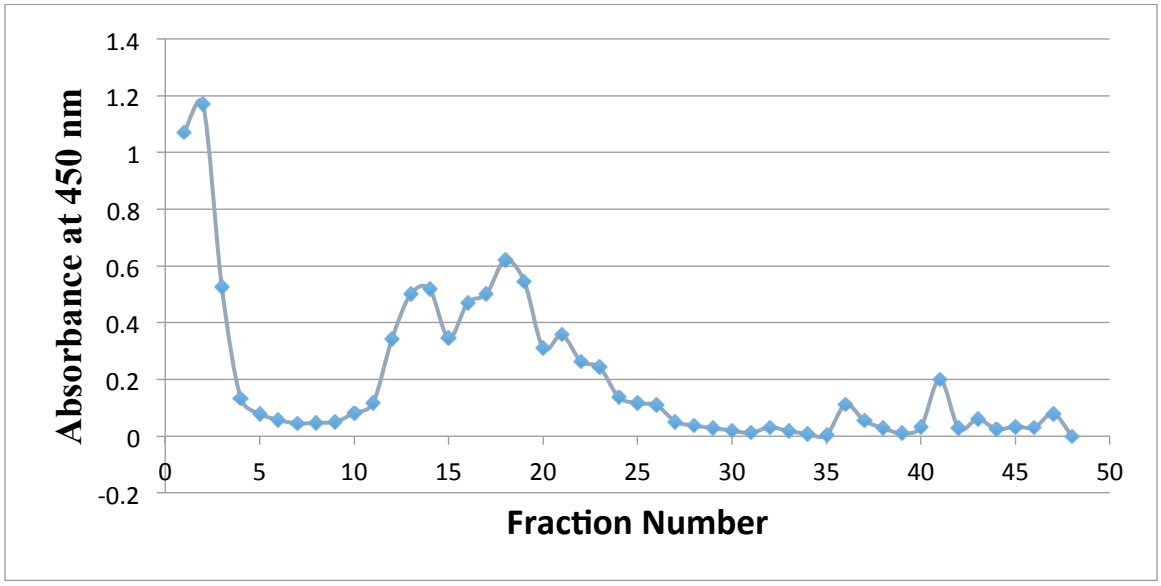

Figure 14. Activity tested by reducing sugar assay for fractions from Mono Q Column 1st run. Adenosine (1mM) reaction mixture + 100 µL of enzyme from Mono Q column 1st run fractions.

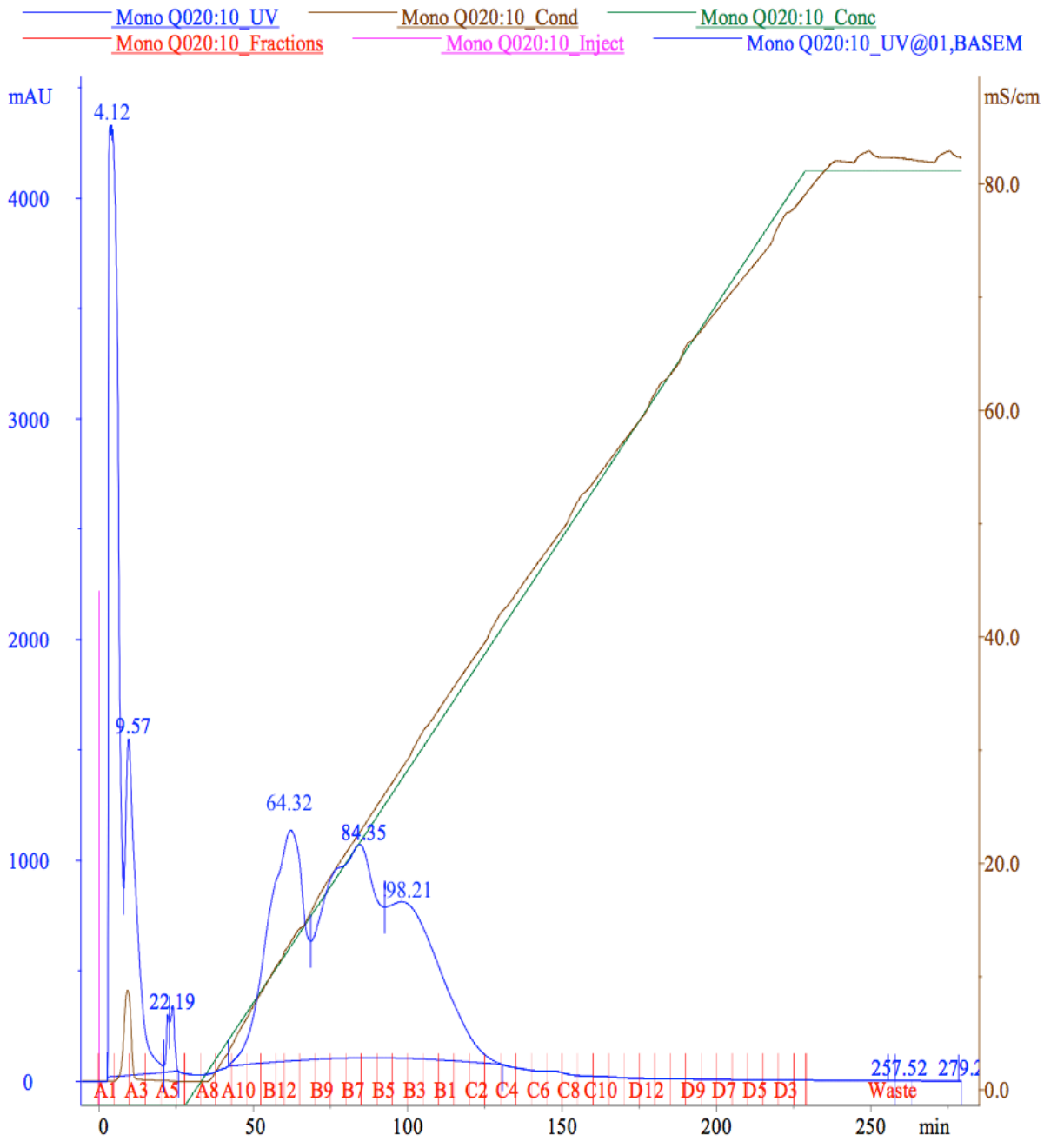

Figure 15. Elution profile (second 5 mL out of 15 mL of total sample) from Mono Q ion exchange chromatography column. The fraction size was 10 mL. Flow rate was 5 mL/min. Two different buffers were used. The low salt buffer, buffer A, was 10 mM Tris buffer pH 7.2, and the high salt buffer, buffer B, was10 mM Tris + 1M NaCl pH 7.2 buffer. A linear gradient from 0% buffer B to 100% buffer B was run over 20-column volume. The gradient started at 50 mL.

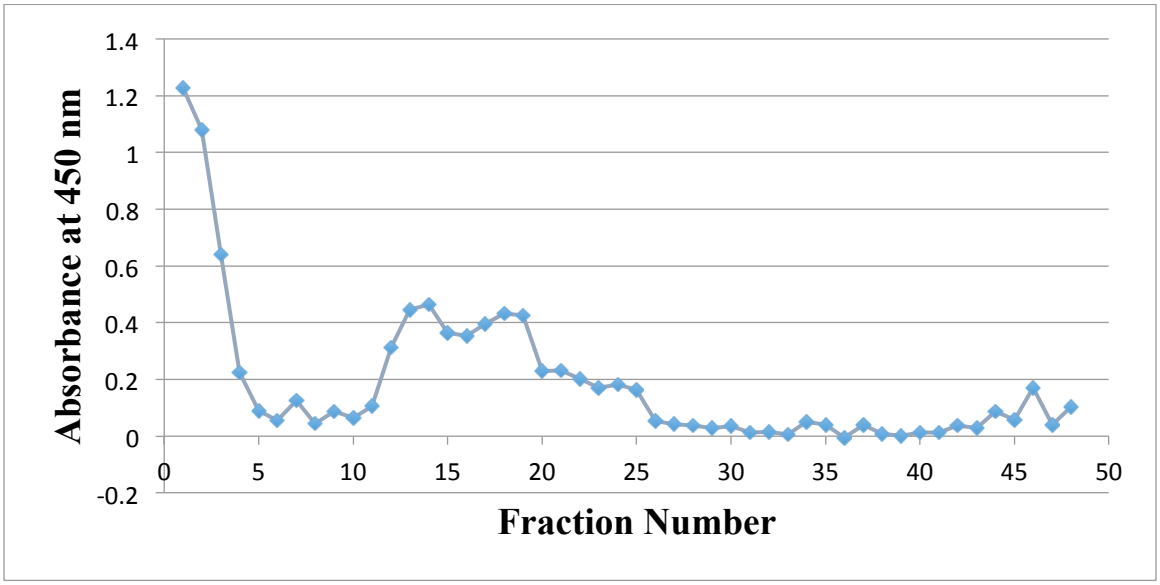

Figure 16. Activity tested by reducing sugar assay for fractions from Mono Q Column 2nd run. Adenosine (1mM) reaction mixture + 100 µL of enzyme from Mono Q column 2nd run fractions.

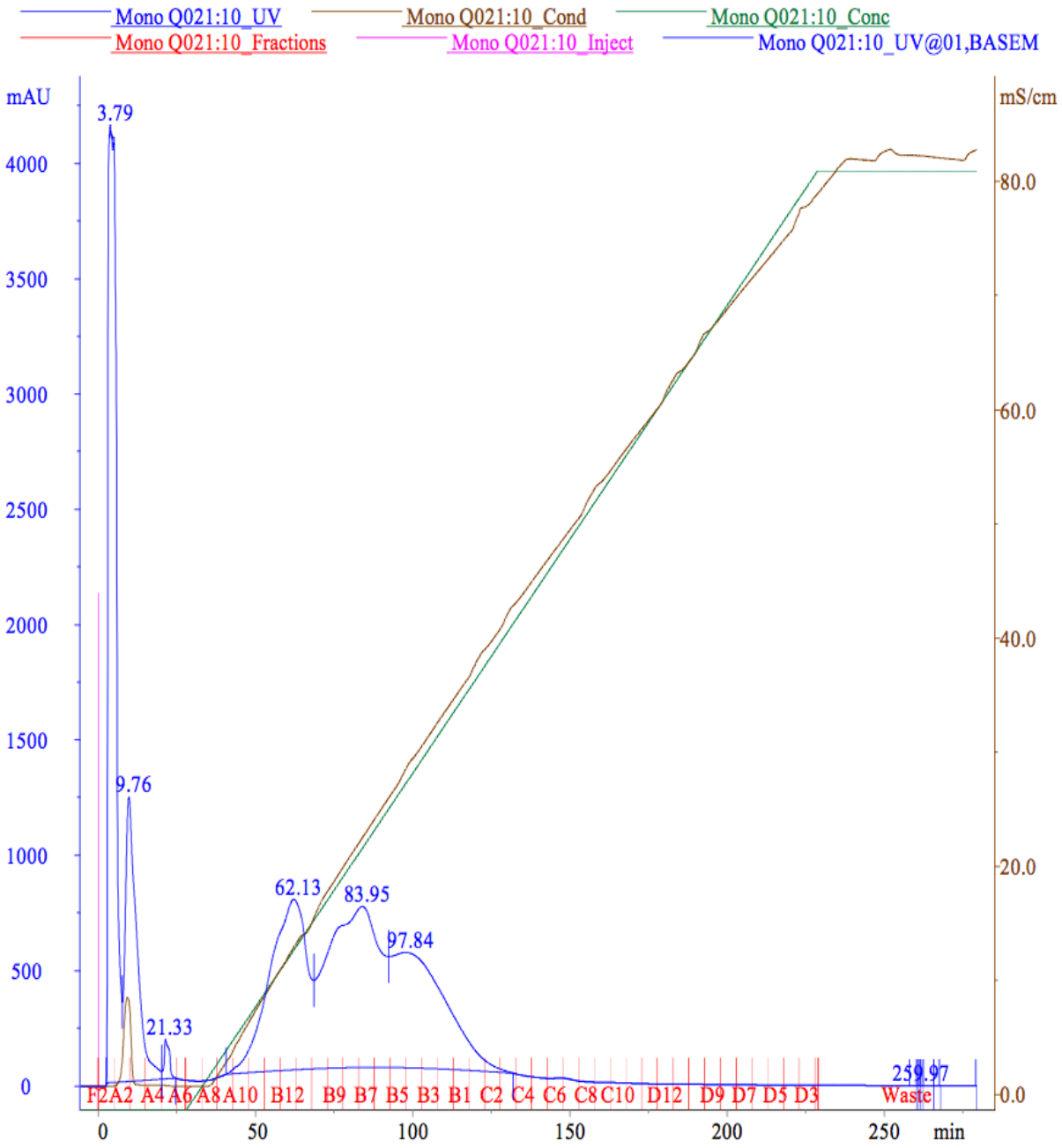

Figure 17. Elution profile (third 5 mL out of 15 mL of total sample) from Mono Q ion exchange chromatography column. The fraction size was 10 mL. Flow rate was 5 mL/min. Two different buffers were used. The low salt buffer, buffer A, was 10 mM Tris buffer pH 7.2, and the high salt buffer, buffer B, was 10 mM Tris + 1M NaCl pH 7.2 buffer. A linear gradient from 0% buffer B to 100% buffer B was run over 20-column volume. The gradient started at 50 mL.

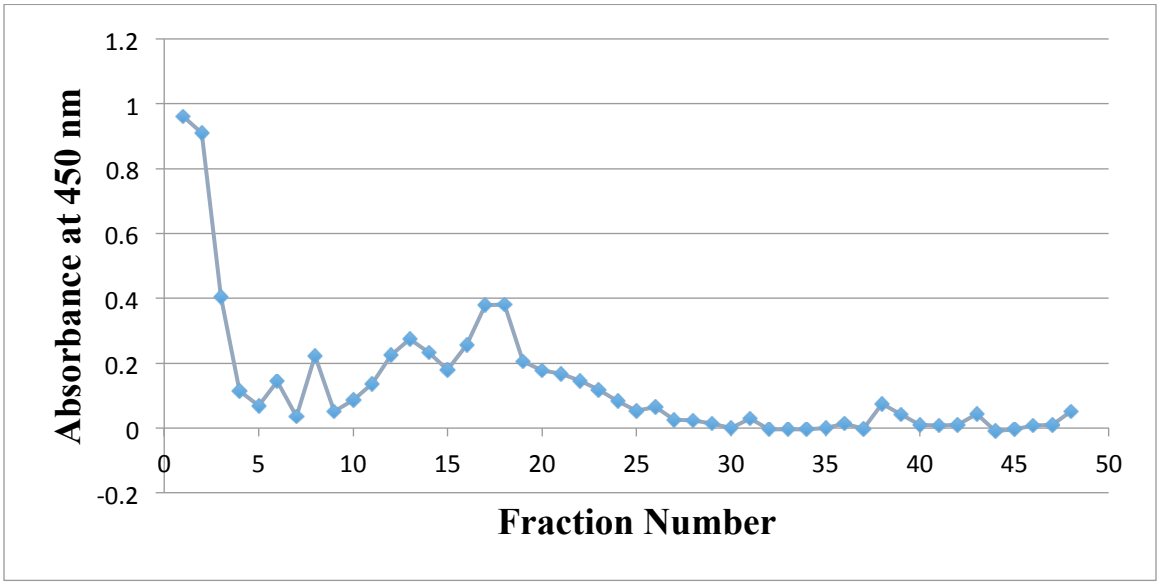

Figure 18. Activity tested by reducing sugar assay for fractions from Mono Q Column 3rd run. Adenosine (1mM) reaction mixture + 100 µL of enzyme from Mono Q column 3rd run fractions.

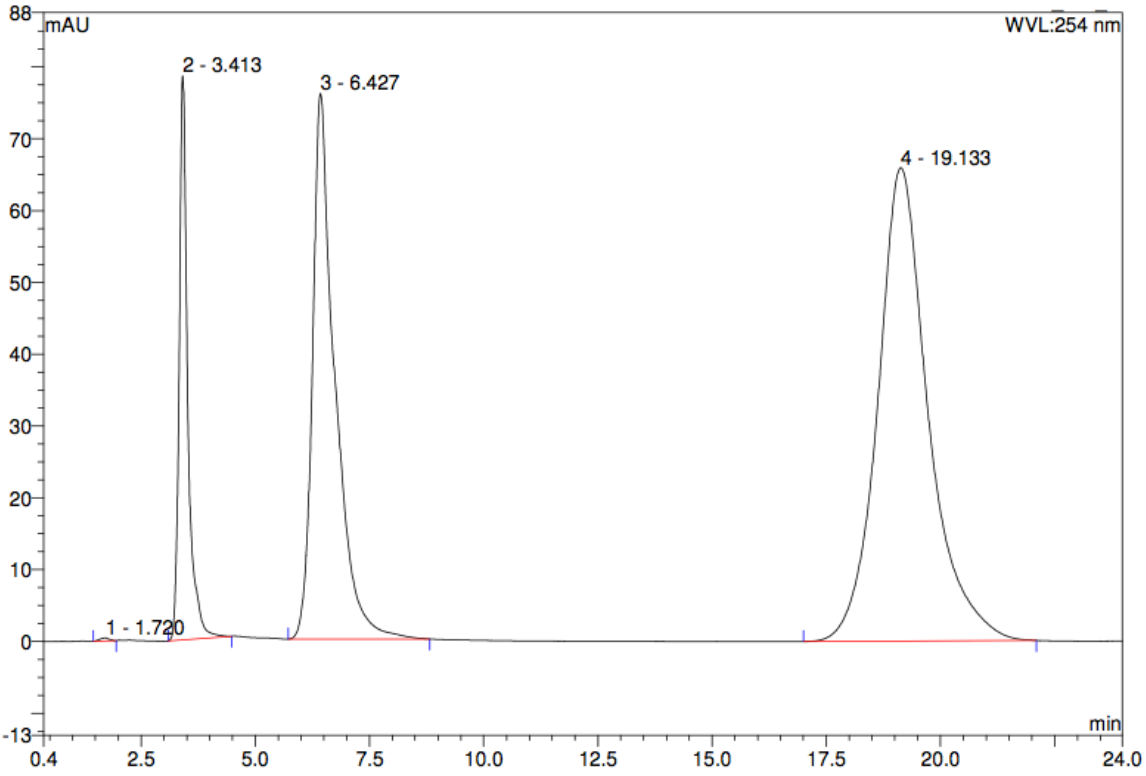

Figure 19. HPLC analysis of activity of pool #1 from Mono Q column. The reaction mixture consisted of 1 mL of 1 mM adenosine in 10 mM Tris pH 7.2. + 50 µL of pool #1 from Mono Q column. After 5 hours, the chromatogram shows adenosine (19.13 min), adenine (6.42 min), and hypoxanthine (3.41 min).

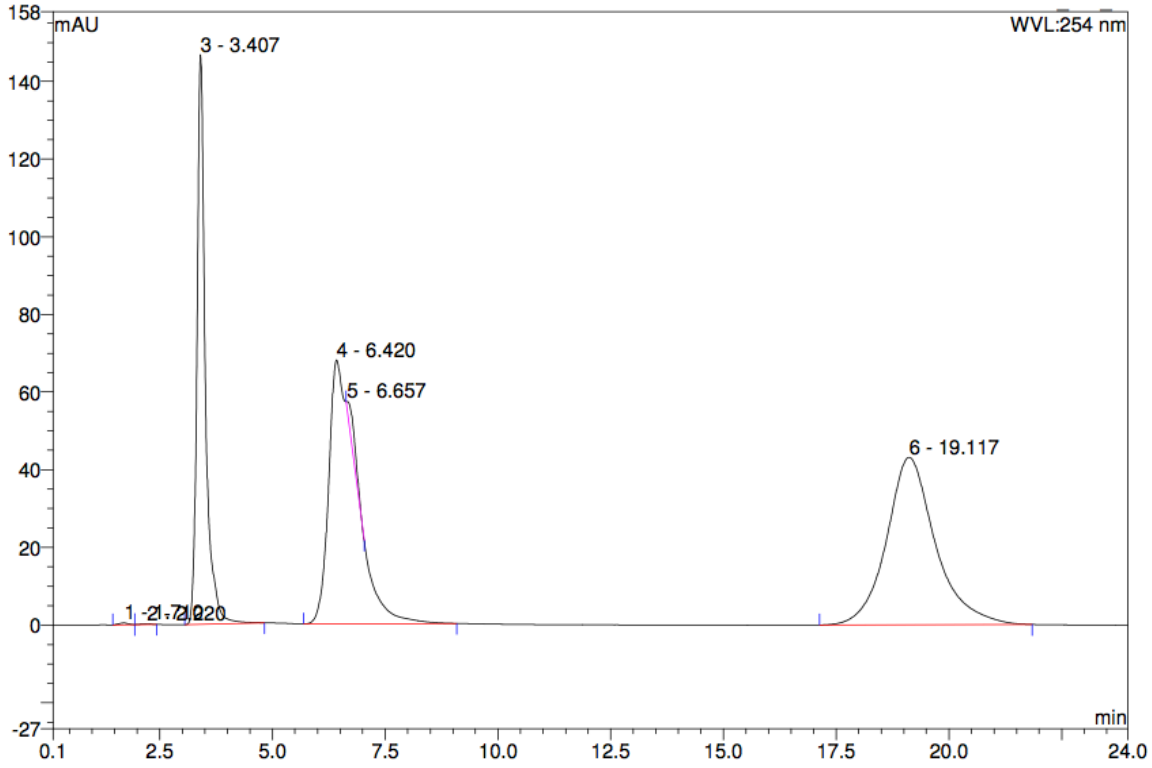

Figure 20. HPLC analysis of activity of pool #2 from Mono Q column. The reaction mixture consisted of 1 mL of 1 mM adenosine in 10 mM Tris pH 7.2. + 50 µL of pool #2 from Mono Q column. After 3.5 hours, the chromatogram shows adenosine (19.13 min), adenine (6.42 min), and hypoxanthine (3.41 min).

The final step of the purification was to use a hydroxyapatite column. This is where this purification differs from earlier purification schemes. The hydroxyapatite column has been traditionally used to isolate nucleic acids such as DNA and RNA, and even though adenosine nucleosidase does not act on nucleic acids, it does bind the individual nucleotides. It was therefore hypothesized that because the substrates of this enzyme are nucleosides, the hydroxyapatite column might further purify the enzyme. Hydroxyapatite is a form of calcium phosphate that has been used in the chromatographic separations of proteins and DNA (*38*). Hydroxyapatite is a crystalline material and is also available in many ceramic derivatives, which are better in terms of flow rate, stability, and reproducibility when they are used many times. Such developments have resulted in a greater interest in the use of this medium with unique separation properties (*38*).

Since the hydroxyapatite involves both anionic and cationic exchange, the adsorption of proteins to it is complicated. The PO_4^{2-} functional group can interact with basic protein residues, while the Ca^{2+} functional group can interact with the carboxylate residues at the protein surface. Proteins are normally adsorbed in a low concentration phosphate buffer (10-25 mM). Some acidic proteins are adsorbed only if loaded in water or a nonphosphate buffer (*38*). Proteins are eluted from the column by increasing the phosphate gradient. Other gradients such as Ca^{2+}, Mg^{2+}, or Cl^- ions are also useful, especially in selectively eluting basic proteins (*38*).

The concentrated samples (pool #1 and pool #2) were loaded onto the hydroxyapatite column. A linear gradient was run from 0 % to 100 % 400 mM potassium phosphate buffer pH 6.8. Multiple peaks were observed in the elution profile of both

samples (Figures 21 and 23). The first peak was eluted in the wash, while the other two were eluted during the linear gradient It was interesting that there were two distinct activity peaks in pool #1, but the activity peaks in pool #2 had an overlap. A reducing sugar assay was done on the fractions collected and the fractions that produced the most ribose were pooled and concentrated (Figures 22 and 24). Fraction numbers 14 – 17 from both runs (pool #1 and pool #2 from hydroxyapatite column) were pooled and named pool #1. Fraction numbers 20 – 23 from both runs (pool #1 and pool #2 from hydroxyapatite column) were pooled and named pool #2. The activities of the pooled samples were tested by HPLC using adenosine as the substrate (Figures 25 and 26). The over all purification after this step was 4-fold with 1.3 % recovery. The specific activity increased to 2.8 $x10^{-2}$ μmol/min/mg. A summary of the purification steps and the calculation results are shown in Table 2.

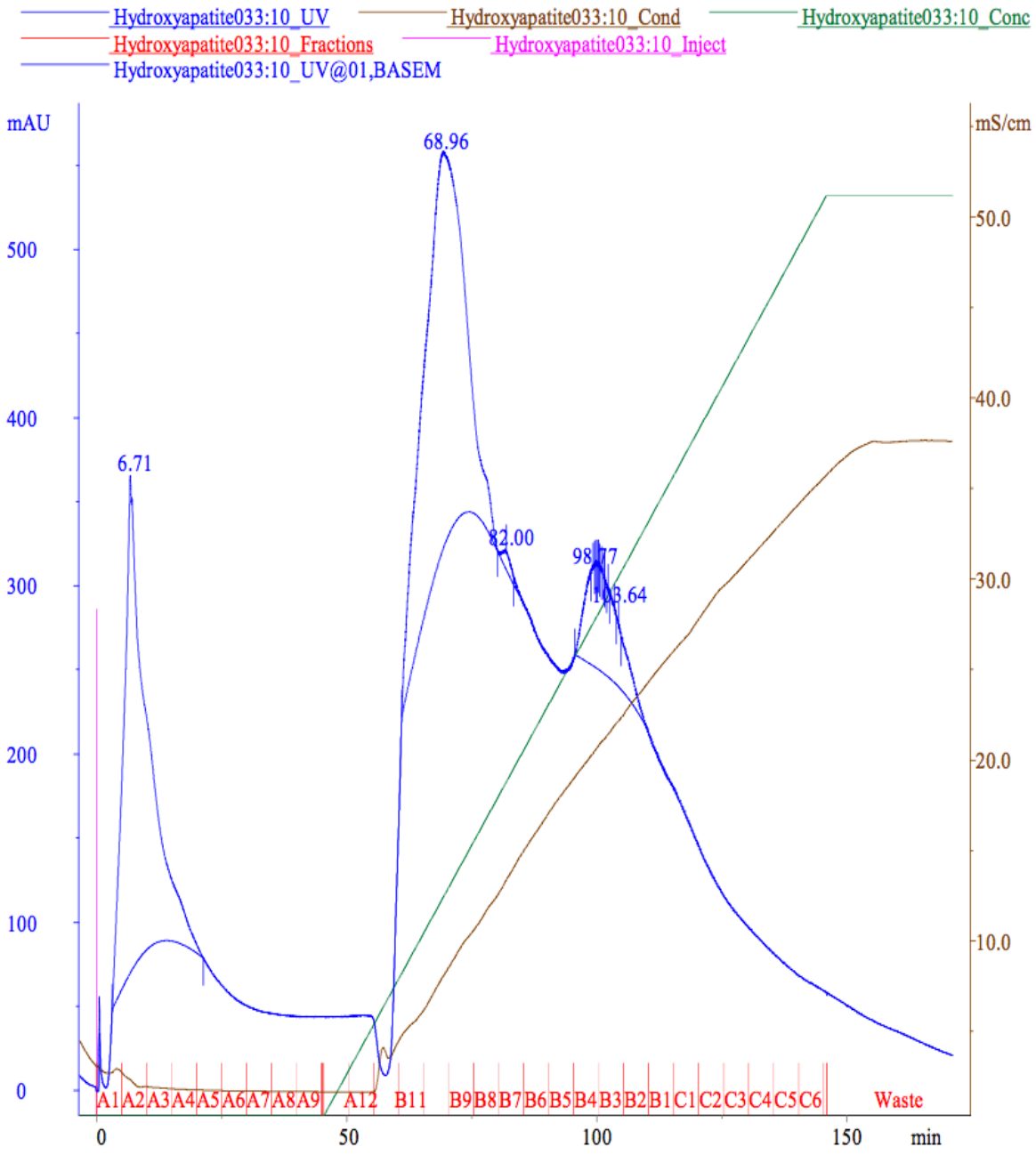

Figure 21. Elution profile (pool #1) from hydroxyapatite chromatography. The column used was BioRad-CHT1- Hydroxyapatite. The flow rate was 1 mL/min. After injecting the sample, the column was washed with six column volumes with low salt buffer. The fraction size was 5 mL. The low salt buffer, buffer A, was 10 mM potassium phosphate buffer pH 6.8, and the high salt buffer, buffer B, was 400 mM potassium phosphate buffer pH 6.8. A linear gradient was run from 0% buffer B to 100% buffer B over 20-column volumes. The gradient started at 50 mL.

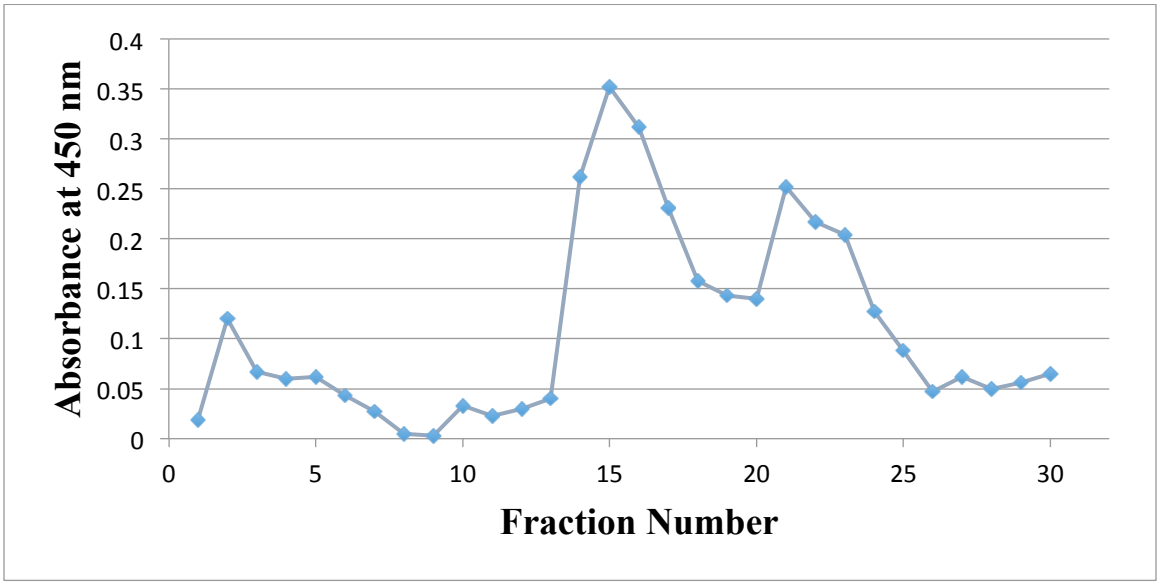

Figure 22. Activity tested by reducing sugar assay for pool #1 from hydroxyapatite column. Adenosine (1mM) reaction mixture + 100 µL of enzyme.

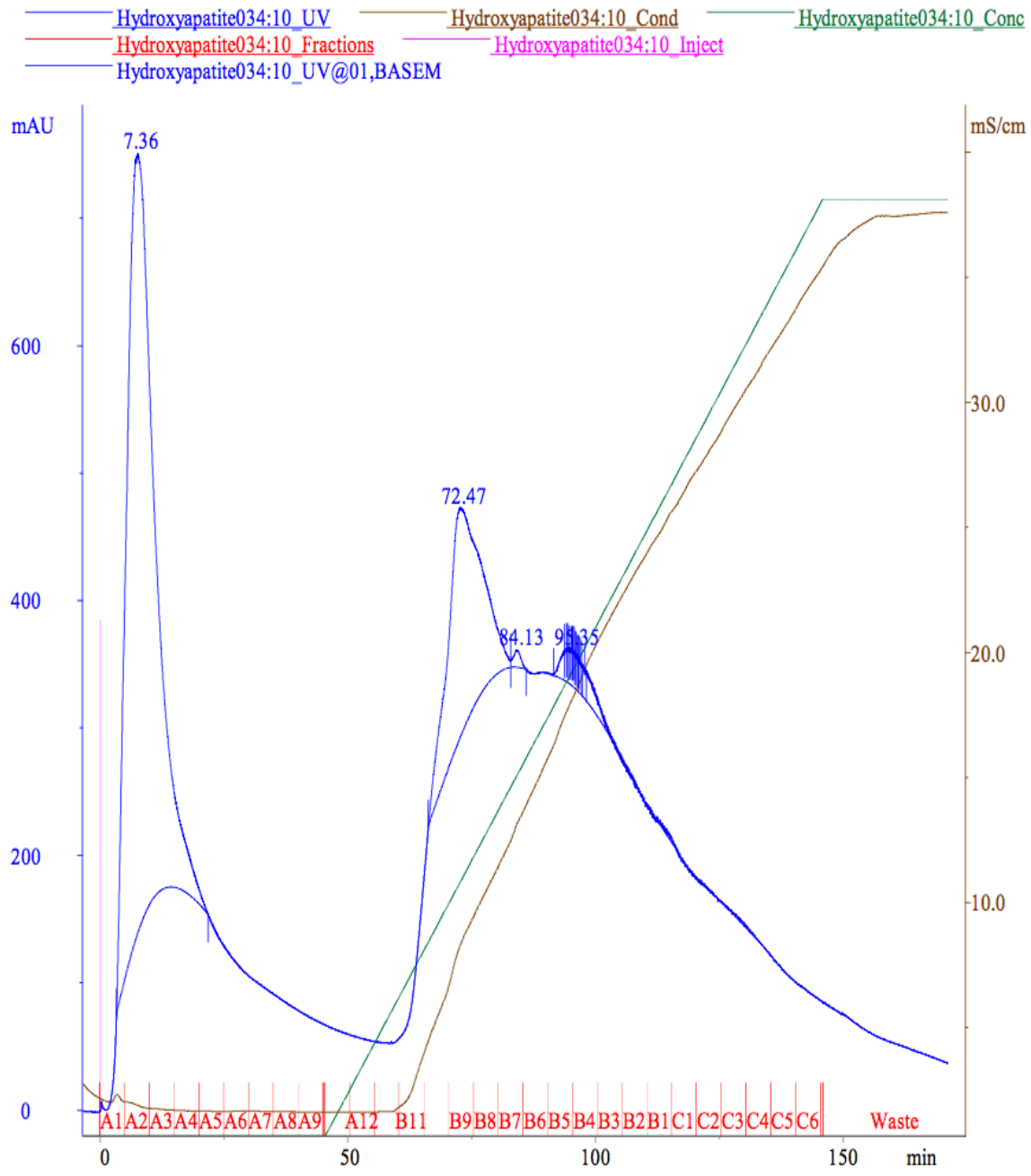

Figure 23. Elution profile (pool #2) from hydroxyapatite chromatography. The column used was BioRad-CHT1-Hydroxyapatite. The flow rate was 1 mL/min. After injecting the sample, the column was washed with six column volumes with low salt buffer. The fraction size was 5 mL. The low salt buffer, buffer A, was 10 mM potassium phosphate buffer pH 6.8, and the high salt buffer, buffer B, was 400 mM potassium phosphate buffer pH 6.8. A linear gradient was run from 0% buffer B to 100% buffer B over 20-column volumes. The gradient started at 50 mL.

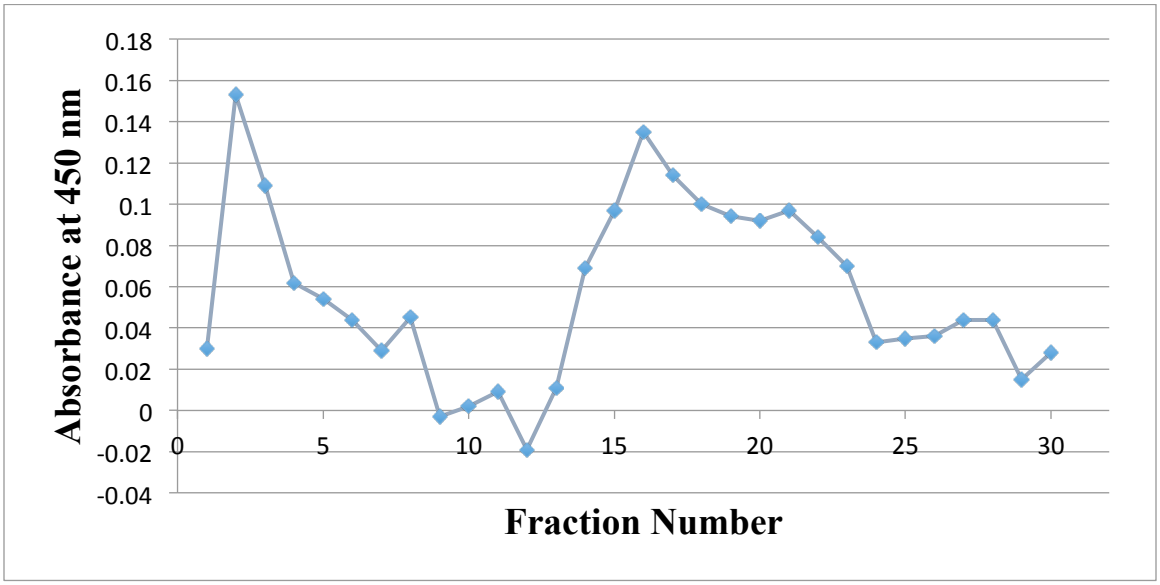

Figure 24. Activity tested by reducing sugar assay for pool #2 from hydroxyapatite column. Adenosine (1mM) reaction mixture + 100 µL of enzyme.

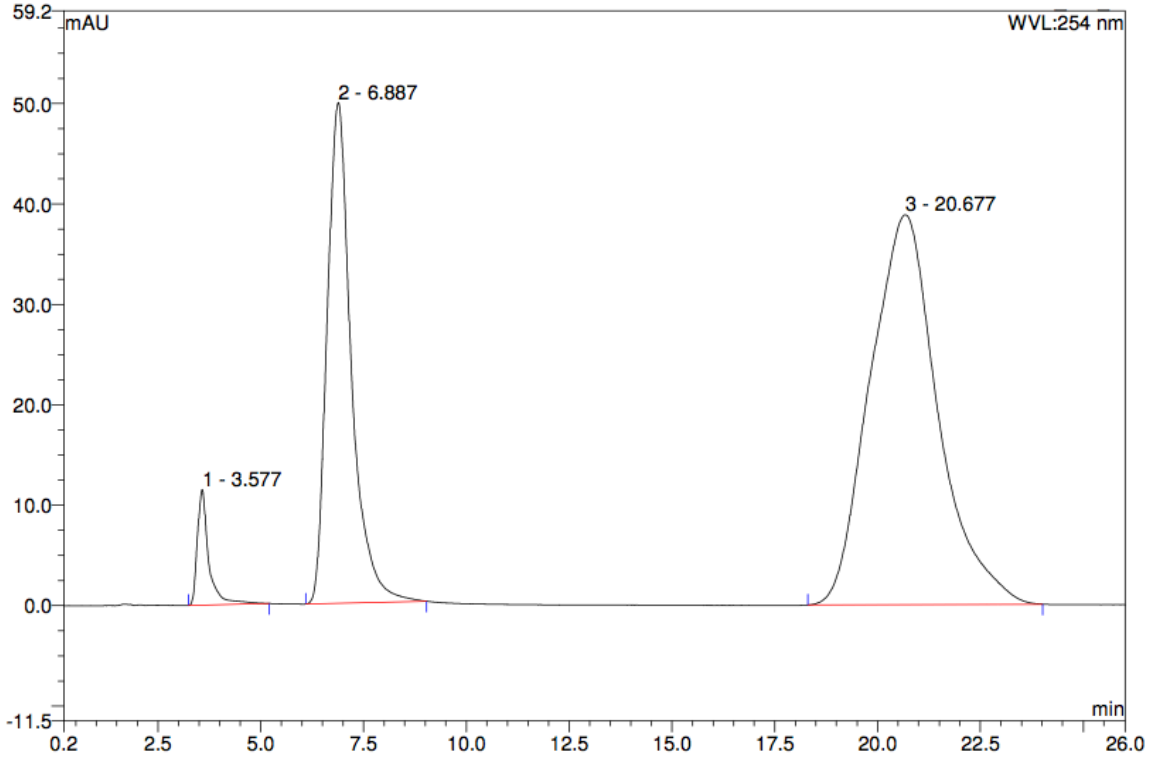

Figure 25. HPLC analysis of activity of pool #1 from hydroxyapatite column. The reaction mixture consisted of 1 mL of 1 mM adenosine in 10 mM Tris pH 7.2. + 100 µL of pool #1 from hydroxyapatite column. After 15 hours, the chromatogram shows adenosine (20.67 min), adenine (6.88 min), and hypoxanthine (3.57 min).

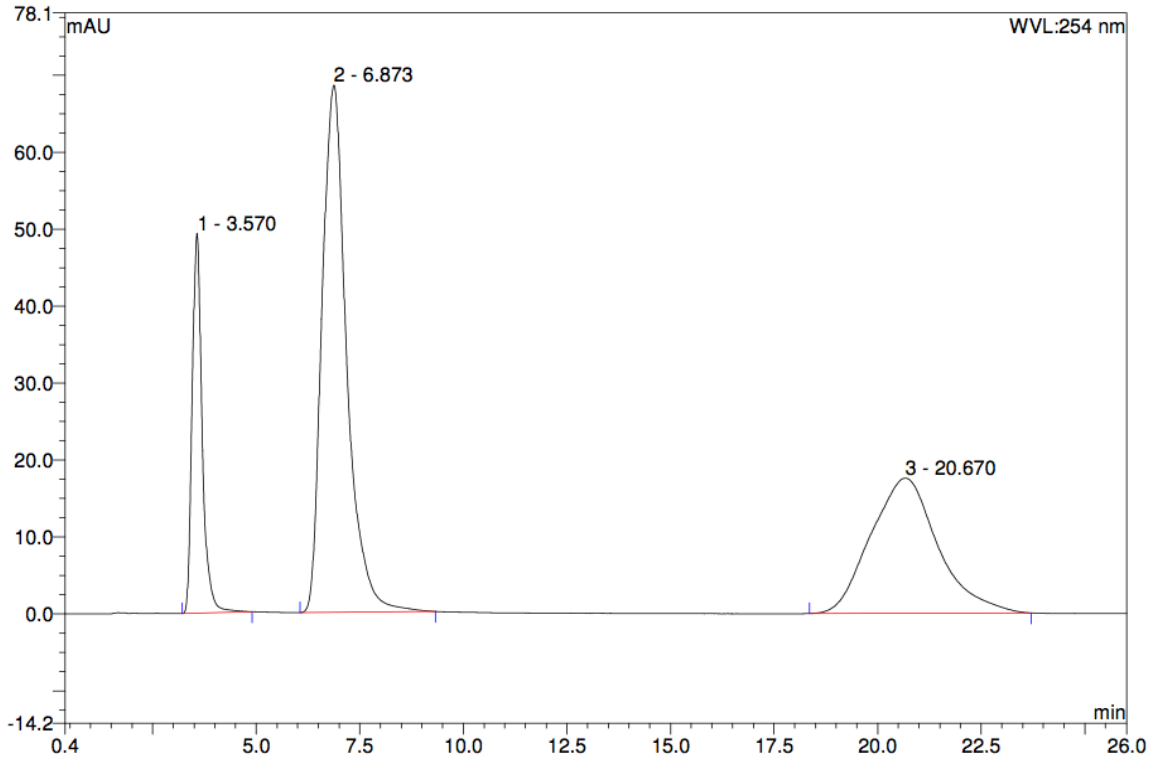

Figure 26. HPLC analysis of activity of pool #2 from hydroxyapatite column. The reaction mixture consisted of 1 mL of 1 mM adenosine in 10 mM Tris pH 7.2. + 100 µL of pool #2 from hydroxyapatite column. After 15 hours, the chromatogram shows adenosine (20.67 min), adenine (6.87 min), and hypoxanthine (3.57 min).

Table 2. Summary of adenosine nucleosidase purification from Alaska pea seeds.

Step	Total Volume (mL)	Protein Concentration ($\mu g/\mu L$)	Total Protein (mg)	Activity (µmol/min)	Total Activity (µmol/min)	Specific Activity (µmol/min*mg)	Purification Fold	% Recovery
Initial Extract	225	5.18	1166.4	$1.9x10^{-3}$	8.55	$7.3\ x10^{-3}$	1	100
Ammonium sulfate 30% Supernatant	240	4.68	1123.92	$1.9\ x10^{-3}$	9.12	$8.1\ x10^{-3}$	1.1	106
Ammonium sulfate 60% Pellet	60	4.92	295.02	$1.3x10^{-3}$	1.56	$5.3x10^{-3}$	0.73	18.3
Mono Q (Ion exchange) (Pool #1)	14	2.35	32.84	$2.4\ x10^{-3}$	0.67	$2.1\ x10^{-2}$	3	7.9
Hydroxyapatite (Pool #2)	12	0.33	3.91	$9\ x10^{-4}$	0.11	$2.8\ x10^{-2}$	4	1.3

Molecular Weight of Adenosine Nucleosidase

The purity and the subunit molecular weight of adenosine nucleosidase were determined by SDS-PAGE. Precision Plus Protein™ Unstained Standards were used to construct a calibration curve, and the calculated subunit molecular weight for both pool#1 and pool #2 was approximately 26,000 daltons. By looking at the gel, the protein appears to be 99% pure (Figures 27 and 28).

In order to obtain a more accurate molecular weight reading, the enzymes were analyzed by electrospray ionization mass spectrometry (ESI-MS). The results showed that both samples, pool #1 and pool #2, are the same enzyme or very close isomers. They molecular weight difference between them was jus 1 daltons. Pool #1 had a molecular weight of 26,104 daltons, and Pool #2 had a molecular weight of 26,103 (Figures 29 and 30).

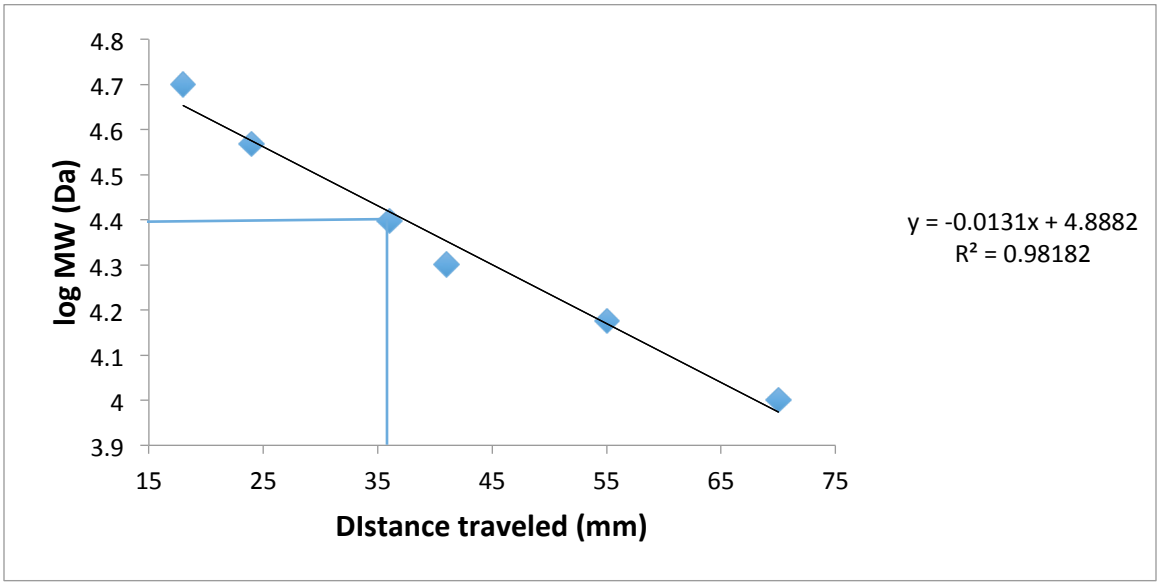

Figure 27. SDS-PAGE molecular weight calibration curve based on the molecular weight of Precision Plus Protein™ unstained standards. The subunit molecular weight for both pool#1 and pool #2 was 26 kDa.

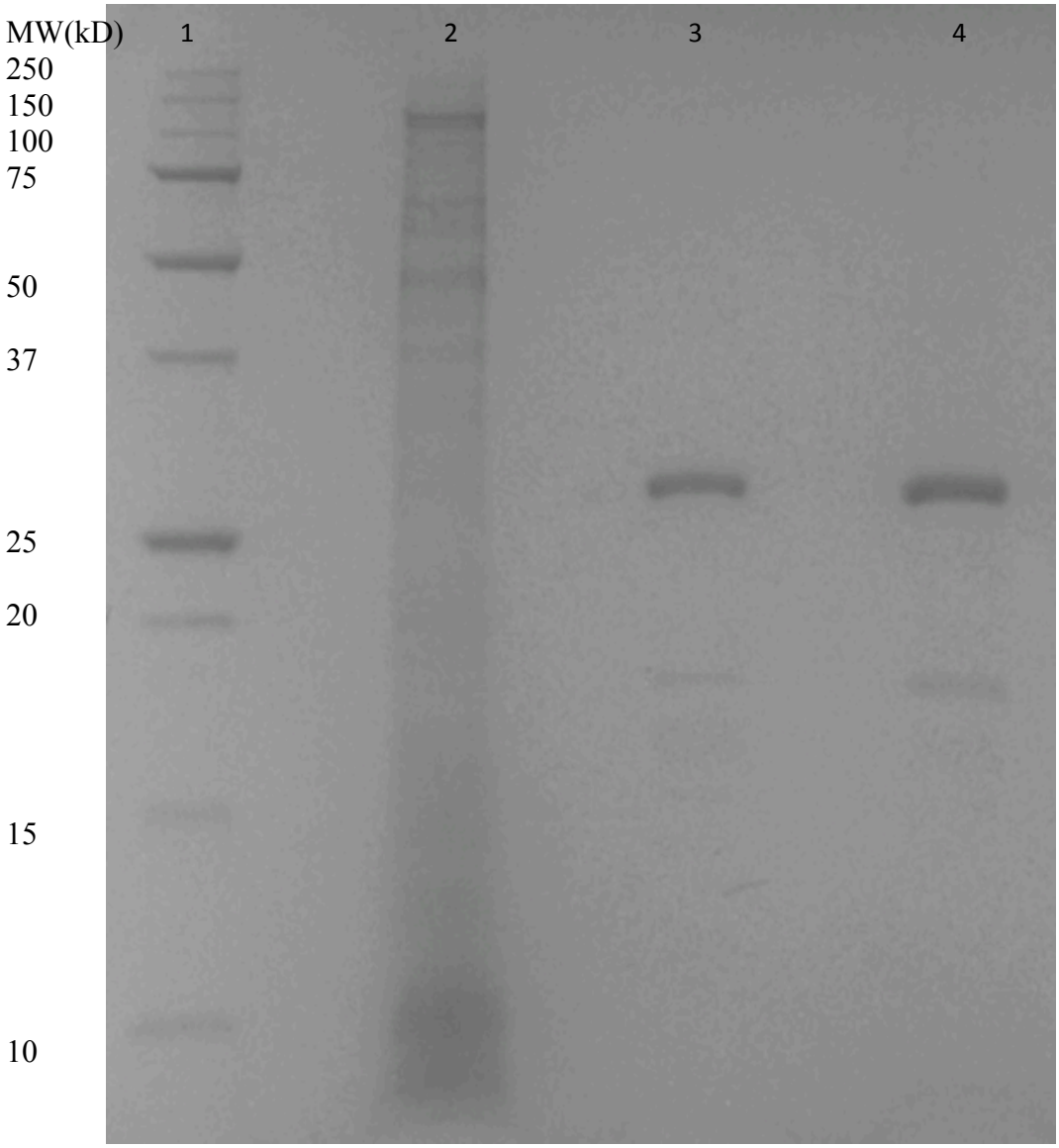

Figure 28. Determination of the subunit molecular weight of adenosine nucleosidase from pool #1 and pool #2 from hydroxyapatite column using SDS-PAGE. Lane 1 is precision plus protein™ unstained markers, and their molecular weights are listed on the left side. Lane 2 is the initial extract of Alaska pea. Lanes 3 and 4 are adenosine nucleosidase pool #1 and pool # 2 respectively from hydroxyapatite column.

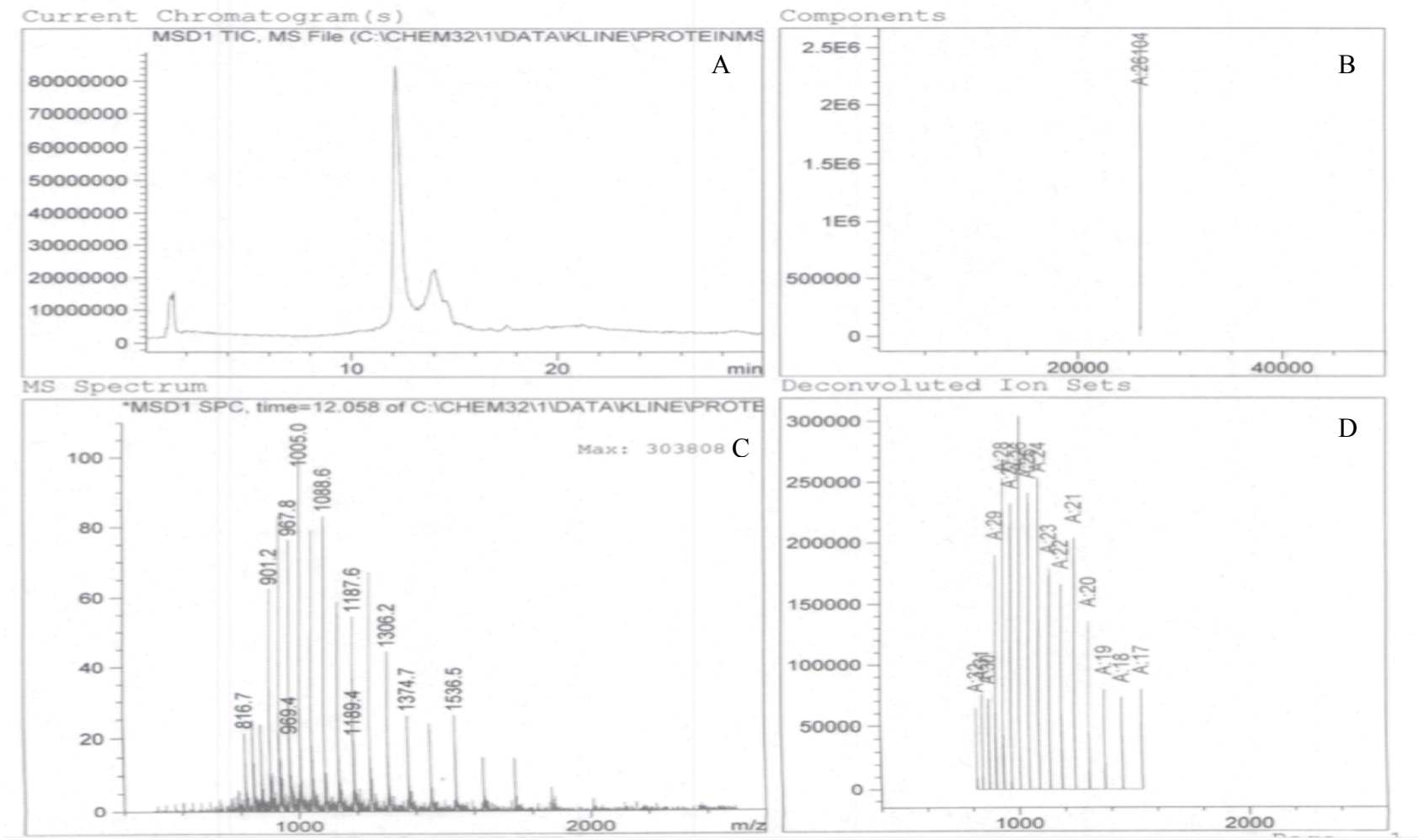

Figure 29. Elution profile of pool # 1 from mass spectrometry. Left to right, (A) current chromatogram, (B) deconvoluted ion sets, (C) MS spectrum, and (D) components. The column used was phenomenex Jupiter C18 300A 5um, 50 x 4.6 mm. Mobile phase A was 0.05% formic acid in water. Mobile phase B was 0.05% formic acid in acetonitrile.

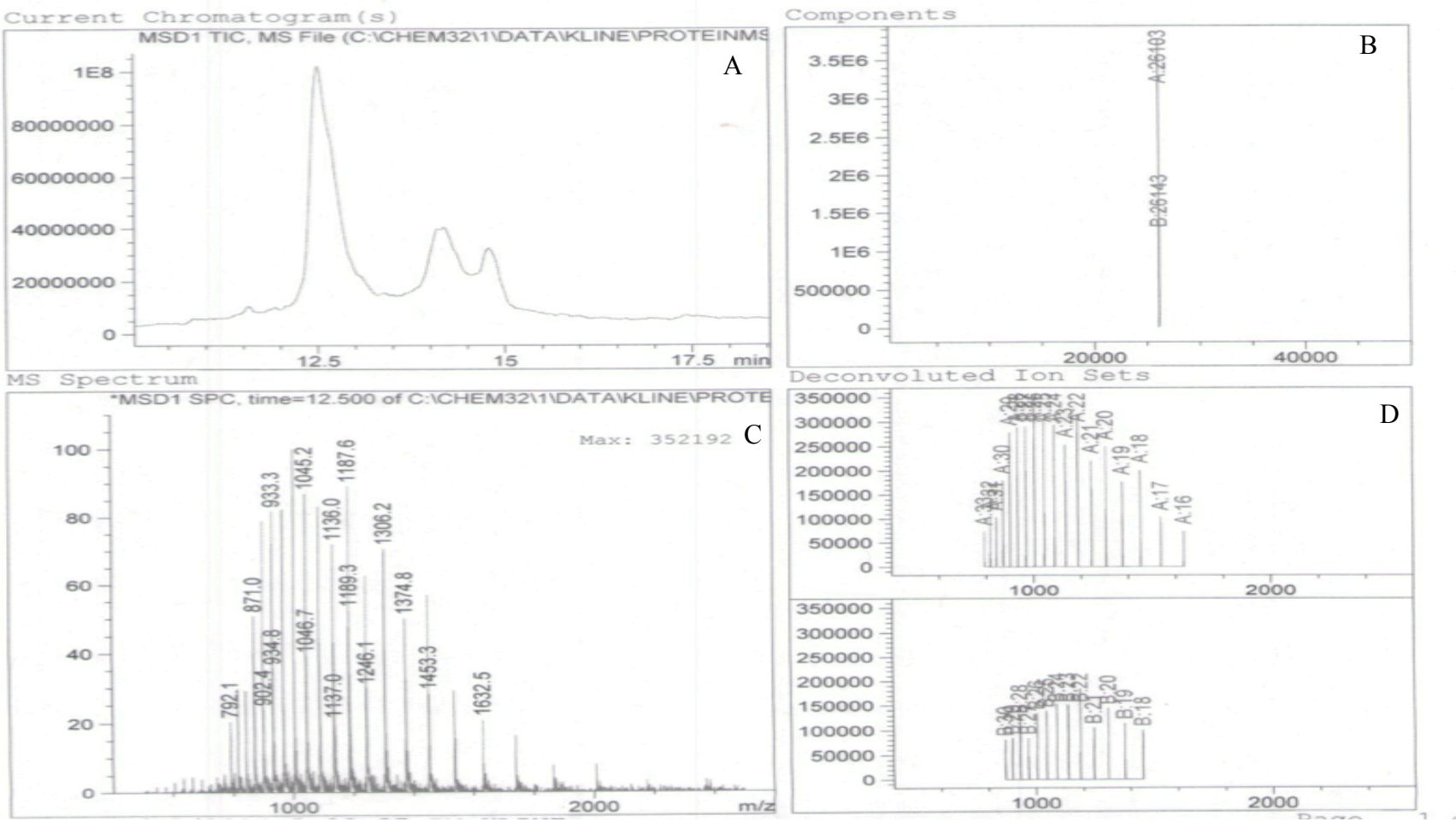

Figure 30. Elution profile of pool # 2 from mass spectrometry. Left to right, (A) current chromatogram, (B) deconvoluted ion sets, (C) MS spectrum, and (D) components. The column used was phenomenex Jupiter C18 300A 5um, 50 x 4.6 mm. Mobile phase A was 0.05% formic acid in water. Mobile phase B was 0.05% formic acid in acetonitrile.

Kinetic Analysis

Enzyme-catalyzed reactions are saturable. As a result, their rate does not show a linear response to increasing substrate concentration above a certain substrate concentration. Many enzymes follow Michaelis-Menten kinetics, which are represented by the Michaelis-Menten equation.

$$V_0 = \frac{V_{\max}[S]}{(K_M + [S])}$$

The velocity of an enzyme-catalyzed reaction depends on the substrate concentration. But at a certain concentration the velocity reaches its maximum value (V_{max}). The Michaelis constant, K_m, can be measured as the substrate concentration at which the velocity of the reaction is half the maximum value. The velocity-substrate concentration profile was determined by measuring the velocity of the reaction at varying substrate concentrations and fitting the data to the Michaelis-Menten equation. A nonlinear regression of a Michaelis Menten plot found the K_m for adenosine to be 137 ± 48 μM, with a V_{max} of 0.34 ± 0.02 μM/min (Figure 31). The assay was run in duplicate.

When comparing the molecular weight and the K_m values of adenosine nucleosidase from Alaska peas to other plant sources (Table 3), it is clear that there are some differences. For example, the molecular weights of adenosine nucleosidase are between 36 and 72 kDa for most sources listed in table 3. On the other hand, adenosine nucleosidase from yellow lupin seeds and malted barley have a molecular weight of 177

and 120 kDa respectively. Altawil (*35*) purified adenosine nucleosidase from Alaska pea seeds and determined the subunit molecular weight by SDS-PAGE to be 36 kDa. In order to accurately determine the molecular weight, the purified enzyme was analyzed by mass spectrometry and the molecular weight from Alaska peas was determined to be 26 kDa.

Adenosine nucleosidase from Alaska peas has a K_m value of 137 ± 48 μM. Comparing this value to the K_m of adenosine nucleosidase from other sources indicates the presence of two groups. The first group, which includes the enzyme from most of the sources listed in Table 3, has a K_m value in the lower range, 0.8-25.0 μM. The second group, which only includes adenosine nucleosidase from malted barley and Alaska pea seeds, has a K_m value greater than 100 μM. A larger K_m value indicates a lower affinity of the substrate for the enzyme. This means it would takes a greater concentration of substrate for the enzyme to be half saturated compared to a low K_m value.

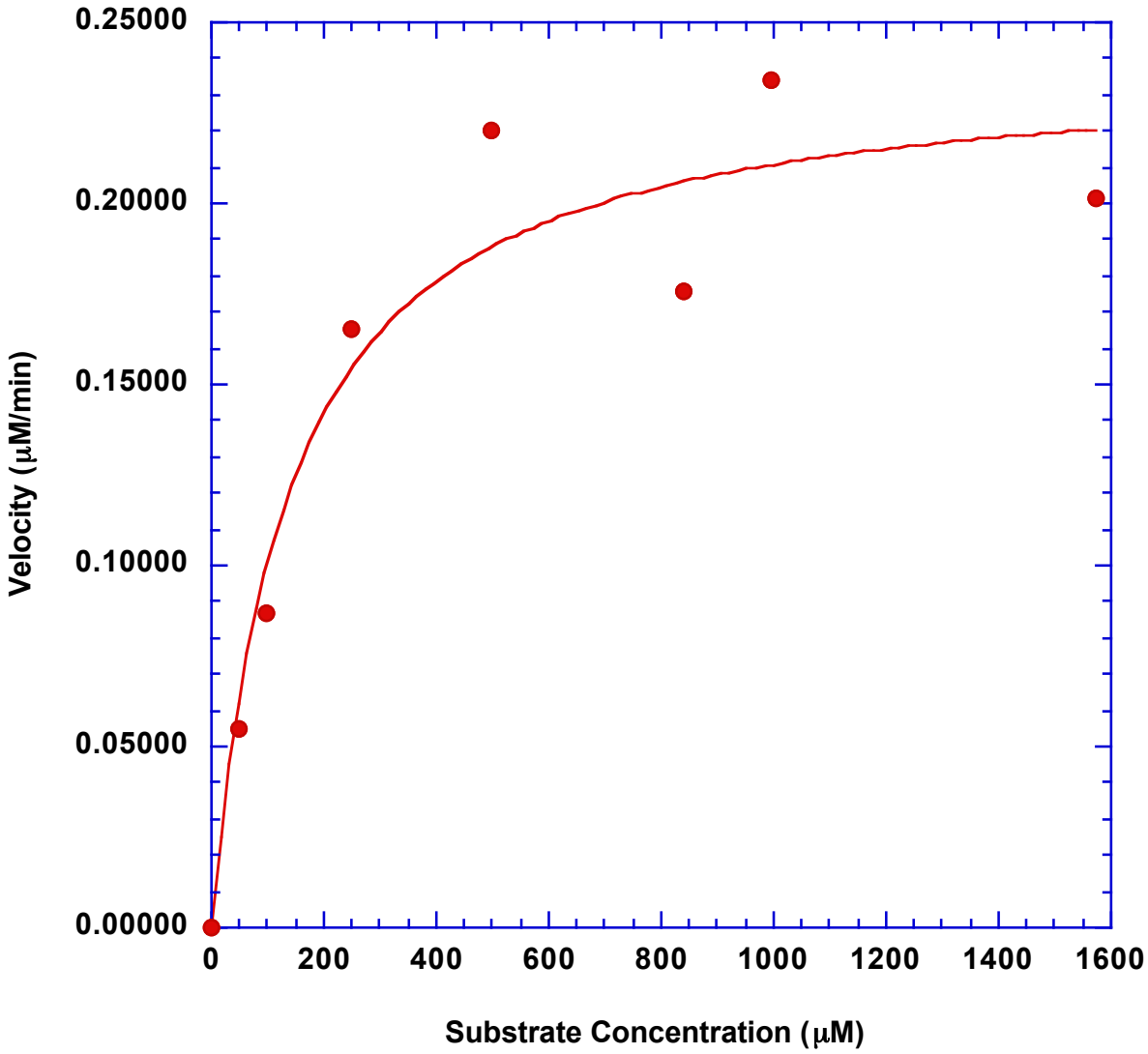

Figure 31. Kinetic analysis of adenosine nucleosidase from Alaska pea seeds. The substrate (adenosine) concentrations used were approximately 50, 100, 250, 500, 850, 1000, and 1500 μM. The Michaelis-Menten equation yields a K_m of 137 ± 48 μM. The assay was run in duplicate.

Table 3. Properties of adenosine nucleosidase from various plant sources.

Tissue	K_m µM	Native Molecular Weight (Da)	Optimum pH	Reference
Yellow lupin seeds	4.7	177,000	7.5	28
Malted Barley	270	120,000	5.0	39
Coffea Arabica young leaves	6.3	72,000	6.0	40
Tomato roots and leaves *R1* *R2* *Lf*	25.0 9.0 6.0	- 68,000 -	5.0 6.0 5.0-6.0	27
Tea leaves	-	68,000	4.0-4.5	24
Barley leaves	0.8-2.3	66,000	4.7-5.4	23
Wheat germ cells	1.43	59,000	4.7	25
Jerusalem artichoke shoots	17	-	5.0-7.0	26
Alaska Pea seeds	-	36,000	-	35
Alaska Pea seeds	137	26,000	-	This Work

Substrate Specificity of Adenosine Nucleosidase

Several substrates were tested for activity against the enzyme purified. Table 4 lists the nucleosides tested and whether they were substrates or not. The reaction mixture consisted of 1 mM nucleoside in 10 mM Tris pH 7.2. The reaction was started by the addition of 25 μL of enzyme. In the control, 25 μL of water was added instead of the enzyme solution. The reaction was incubated 15 hours in the HPLC. Whether a nucleoside was a substrate or not was determined by the production of the base in the reaction mixture of the nucleoside and the enzyme solution. This was the way all of the substrate specificity tests were done in the HPLC. The activity was measured by separating the nucleoside from the base. The peak area represented how much of each one was there, and as a function of time, that was the velocity. Any nucleoside that hade greater than 20% conversion from nucleoside to base was classified as a substrate. All of these nucleosides were run at 1 mM and it is assumed that this is two times K_m, which means the velocities are at V_{max}.

Based on the observed substrate specificity, adenosine nucleosidase from Alaska pea seeds hydrolyze both purines and pyrimidines. This indicates that it belongs to the non-specific inosine-uridine nucleoside hydrolases (IU-NHs). Some of the nucleosides were used to test the effect of structural features on enzyme activity. Usually the number and position of the hydroxyl groups on the ribose in a nucleoside are important in determining the substrate specificity, but this was not the case with adenosine nucleosidase from Alaska pea. For example, uridine is a substrate for adenosine nucleosidase, while uracil-1-β-D-arabino-furanoside is not. When comparing their

structures, both uridine and uracil-1-β-D-arabino-furanoside have a hydroxyl group in the 2’ position, but uracil-1-β-D-arabino-furanoside has the opposite stereochemistry from that of uridine (Figure 32). This means the hydroxyl group in uracil-1-β-D-arabino-furanoside has to have the same stereochemistry as uracil for the enzyme to work. On the other hand, the difference between thymidine and 5-methyluridine is the absence of a hydroxyl group in the 2’position in thymidine, yet both nucleosides act as substrates for the enzyme (Figure 33).

Table 4. Substrate specificity of adenosine nucleosidase. “Yes” represents the nucleosides that had greater than 20% conversion of nucleoside to base and they were classified as a substrate.

Nucleoside	**Substrate**	**Nucleoside**	**Substrate**
Adenosine	*Yes*	2'-Deoxyadenosine	*Yes*
Guanosine	*No*	3'-Deoxyadenosine (Cordycepin)	*Yes*
Inosine	*Yes*	5'-Deoxyadenosine	*Yes*
Uridine	*Yes*	7-Deazaadenosine (Tubercidin)	*No*
Cytidine	*Yes*	5-Methyluridine	*Yes*
Thymidine	*Yes*	Uracil-1-β-D-arabino-Furanoside	*No*
		Purine Riboside	*No*

The conclusion that this enzyme is not selective for the number and position of the hydroxyl groups on the ribose in a nucleoside that acts as a substrate is supported by the fact that 2’-deoxyadenosine, 3’-deoxyadenosine, and 5’-deoxyadenosine are substrates. 2’-Deoxyadenosine lacks the hydroxyl group in the 2’ position, yet it acts as a substrate (Figure 34). 3’-Deoxyadenosine, and 5’-deoxyadenosine are substrates even though both lack a hydroxyl group at different carbons (Figure 35 a and b).

Certain structural features of the base were critical for the reaction between the enzyme and the substrate. The generally accepted mechanism for purine hydrolysis by the nucleoside hydrolases is that an amino group will protonate the nitrogen in the N7 position and help turn the ribose into a better leaving group. Since in 7-deazaadenosine the nitrogen in the N7 position has been replaced with a carbon (Figure 36), 7-deazaadenosine should not be a substrate. This is observed with the enzyme purified and it follows the generally accepted mechanism of N7 protonation. Also of prime importance is the free amino group at the N6 position on the purine ring. When the amino group is moved to the C_2 position of the purine ring, as in the case of guanosine, no reaction takes place (Figure 37).

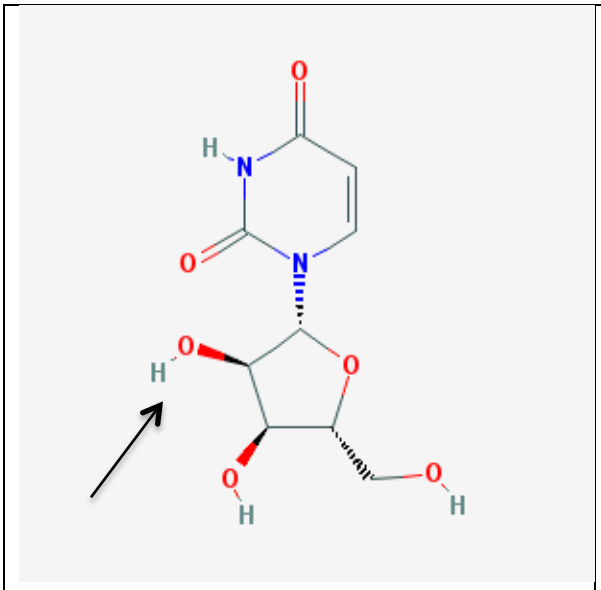

Uridine (Substrate)	Uracil-1-β-D-arabino-furanoside (Not a substrate)

Figure 32. Structure of uridine and uracil-1-β-D-arabino-furanoside (*41*).

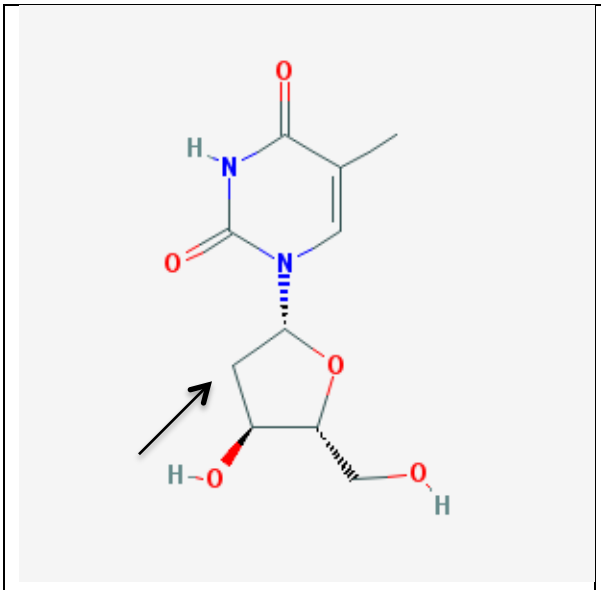

Thymidine (Substrate)	5-Methyluridine (Substrate)

Figure 33. Structure of thymidine and 5-methyluridine (*41*).

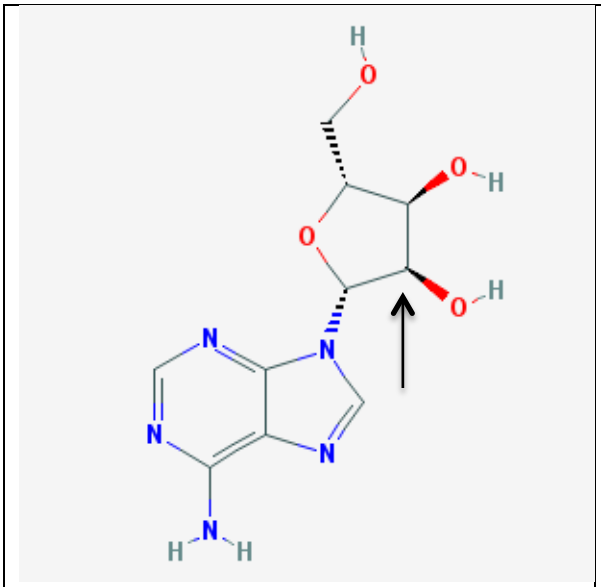

Adenosine (Substrate)	2’-Deoxyadenosine (Substrate)

Figure 34. Structure of adenosine and 2’-deoxyadenosine (*41*).

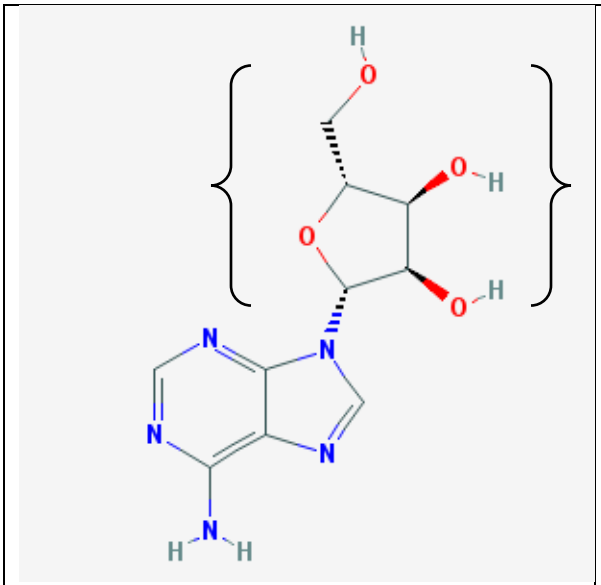

Adenosine (Substrate)	3’-Deoxyadenosine (Substrate)

Figure 35a. Structure of adenosine and 3’-deoxyadenosine (*41*).

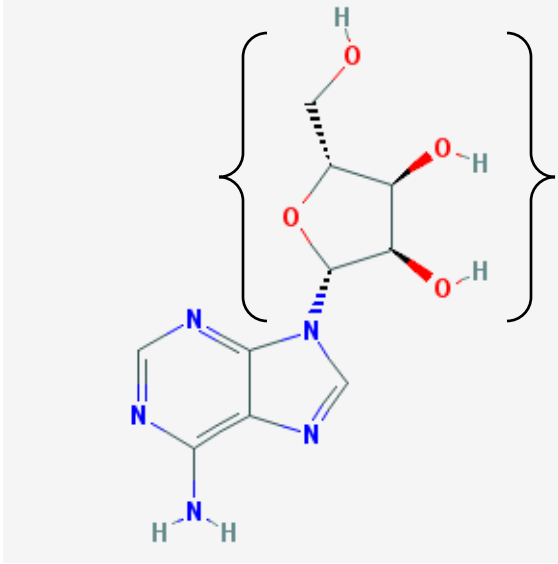

Adenosine (Substrate)	5’-Deoxyadenosine (Substrate)

Figure 35b. Structure of adenosine and 5’-deoxyadenosine (*41*).

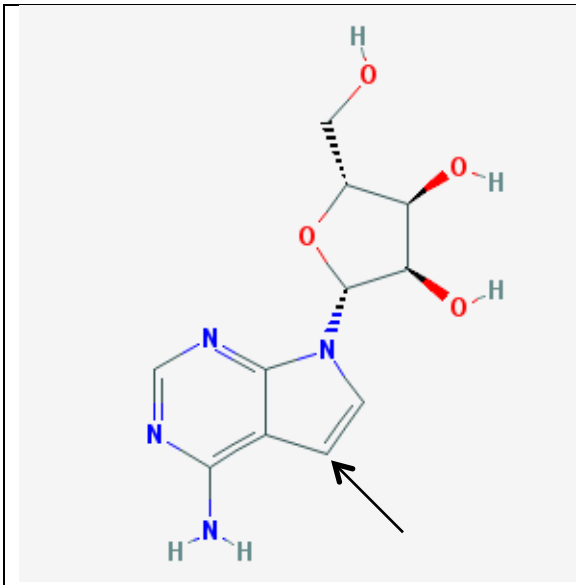

7-Deazaadenosine (Not a substrate)	Adenosine (Substrate)

Figure 36. Structure of 7-deazaadenosine and adenosine (*41*).

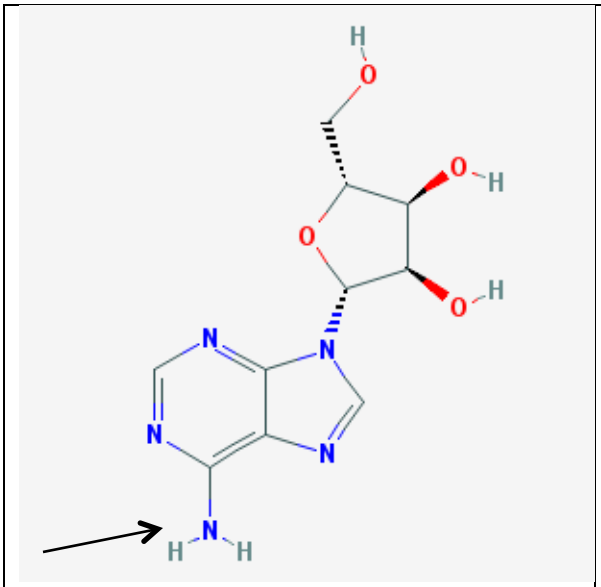

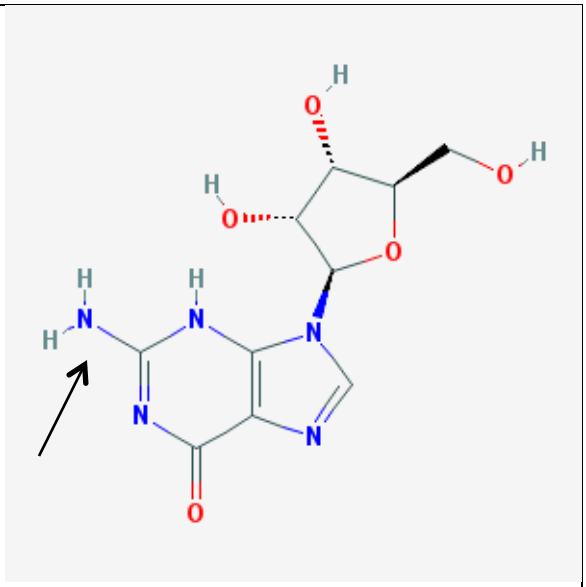

Adenosine (Substrate)	Guanosine (Not a substrate)

Figure 37. Structure of adenosine and guanosine (*41*).

Comparing the substrate specificity of adenosine nucleosidase from various plant sources (Table 5) suggests many similarities and differences between all the plant sources, including Alaska pea seeds. For example, adenosine nucleosidase from Jerusalem artichoke shoots, wheat germ cells, barley leaves, and tea leaves were specific for purines, while adenosine nucleosidase from yellow lupin seeds, similar to that of Alaska pea seeds, reacted with both purines and pyrimidines. The enzyme from Alaska pea seeds was somewhat similar to the enzyme from barley leaves, tea leaves, and yellow lupin seeds in that they all had a form of deoxyadenosine as a substrate. However, the enzyme from Alaska pea seeds was the only one that had 2', 3', and 5'-deoxyadenosine as substrates.

Table 5. Substrate specificity of adenosine nucleosidase from other plant sources.

Adenosine Nucleosidase Plant Source	Nucleoside tested for activity	Substrate	Reference
Jerusalem artichoke shoots	Adenosine Inosine Guanosine	Yes Yes Yes	26
Wheat germ cells	Adenosine N^6-derivatives of adenosine Guanosine Uridine 3'-Deoxyadenosine	Yes Yes No No No	25
Barley leaves	Adenosine Deoxyadenosine Adenosine N_1-oxide Purine riboside Guanosine Inosine Uridine Cytidine Thymidine	Yes Yes Yes Yes No No No No No	23
Tea leaves	Adenosine 2'-Deoxyadenosine Adenosine N_1-oxide Guanosine Inosine Uridine Cytidine Thymidine 3'-Deoxyadenosine	Yes Yes Yes No No No No No No	24
Yellow lupin seeds	Adenosine Deoxyadenosine Guanosine Cytidine Thymidine Inosine	Yes Yes Yes Yes Yes Yes	28

This is different from the other enzyme, and it implies that neither the 2’ nor the 3’ hydroxyl groups are necessary for the reaction to take place.

Extracts from a wide range of protozoan parasites indicates the presence of several nucleoside hydrolases with different substrate specificity (*42*). Two nucleoside hydrolases were detected in *Trypanosoma cruzi* (*42*). One of the nucleoside hydrolases was designated inosine/guanosine hydrolase. It was specific for purine substrates containing 9-β-D-ribofuranosyl. Inhibition studies with several deoxyinosines have shown the prime importance of the hydroxyl groups on the 2’, 3’, and 5’ positions for enzyme activity (*42*). This is different from enzyme purified from Alaska pea seeds in which the position of the hydroxyl groups were not important and did not affect the activity of the enzyme. The second nucleoside hydrolase from *Trypanosoma cruzi* only reacted with 2’-deoxyinosine.

Two enzymes were discovered in C. *fasciculata*. The most abundant nucleoside hydrolase favors inosine and uridine as substrates (IU-NH), but also catalyzes the hydrolysis of all commonly occurring purine and pyrimidine nucleosides. The second enzyme is extremely active with guanosine and inosine, but inert with pyrimidine nucleosides and adenosine(*43*). The nucleoside hydrolase (IU-NH) from C. *fasciculata* showed no activity toward deoxynucleosides. Deoxynucleosides at the 2’, 3’, and 5’ positions were poor substrates or they lacked substrate activity (*43*). This is different from the enzyme purified from Alaska pea seeds in which the deoxynucleosides at the 2’, 3’, and 5’ positions were all substrates.

Three different nucleoside hydrolases with very distinct catalytic and physical properties were purified from *Leishmania donovani* (*44*). The first nucleoside hydrolase (native molecular weight 33,000 daltons) had a strict substrate specificity for purine 2'-deoxyribonucleosides. The second hydrolase (native molecular weight 205,000 daltons) was specific for purine ribonucleosides. Inosine and guanosine were both substrates, but not adenosine and xanthosine. The third hydrolase (native molecular weight 180,000 daltons) was non-specific reacting with both purines and pyrimidines with preference for pyrimidines (*44*).

Nucleoside hydrolase from *Trypansosma vivax* is a member of the inosine adenosine guanosine preferring nucleoside hydrolase (IAG-NH) (*16*). The enzyme is 1000 to 10,000 times more specific toward naturally occurring purine nucleosides as compared to pyrimidine nucleosides. Nucleoside hydrolase from *Trypansosma brucei brucei*, also a member of the IAG-NH, has also showed specificity toward purine nucleoside hydrolases (*45*).

When comparing the substrate specificity of the nucleoside hydrolases from the protozoan parasites mentioned above to that of the purified enzyme, some similarities yet significant differences are observed. For example, one of the enzymes in C. *fasciculata* hydrolyze all commonly occurring purine and pyrimidine nucleosides as does the enzyme purified from Alaska pea seeds. Three different nucleoside hydrolases were purified from *Leishmania donovani*. One of those enzymes (native molecular weight 180,000 daltons) was similar to the enzyme purified from Alaska pea seeds because it was non-specific and reacted with both purines and pyrimidines. On the other hand, nucleoside hydrolases

from *Trypansosma vivax* and *Trypansosma brucei brucei* were members of the IAG-NH and were specific for purine nucleoside hydrolases.

The difference between the parasitic protozoa enzymes and the purified enzyme from Alaska pea seeds was the ability to hydrolyze deoxyribonucleosides. Deoxynucleosides at the 2', 3', and 5' positions were poor substrates or lacked substrate activity with the nucleoside hydrolase from C. *fasciculata*. Also, even though one of the nucleoside hydrolase from *Leishmania donovani* (native molecular weight 33,000 daltons) reacted with deoxyribonucleosides, it had a strict substrate specificity for purine 2'-deoxyribonucleosides and not 3', 5'- deoxyribonucleosides. This is completely different from the purified enzyme in which 2', 3', and 5'-deoxyadenosine were substrates. Also, this difference indicates that there might be a difference in the reaction mechanism between these enzymes.

The reported mechanism for nucleoside hydrolases specified that NHs have one active site per subunit. At the bottom of the active site, there is a Ca^{2+} ion that is tightly bound (Figure 7) (*16*, *20*). Once the substrate binds, the ribose moiety is secured inside the active site cleft (*4*). After the complex is formed, two Ca^{2+}-bound water molecules are substituted with the 2'-and 3'-hydroxyl groups of the sugar. The last remaining Ca^{2+}-chelated water molecule interacts with aspartate (Asp10). The basis of the strict specificity of the NHs for ribose is found in the complex network of interactions that involves the 2'-, 3'- and 5' hydroxyls of the sugar and Asp14, Asn173, Glu184, Asn186 and Asp261 (*Tv*NH numbering), and the Ca^{2+} ion (Figure 7).

Comparing this mechanism to the substrate specificity result of the purified enzyme shows clearly that the purified enzyme (adenosine nucleosidase from Alaska pea seeds) follows a different mechanism. This observation is reinforced by the fact that not only is 2’-deoxyadenosine a substrate, but 3’-deoxyadenosine (cordycepin) is a substrate as well (Figure 38). These results suggest that the reaction mechanism is different because for the purines it doesn’t appear that the hydroxyl group in either the 2’ position or in the 3’ position is necessary for the reaction. This is completely different from the parasitic protozoa inosine uridine nucleoside hydrolase (IU-NH), in which the hydroxyl groups coordinate the reaction. Since the three dimensional structure and binding modes of the purified enzyme are not yet known, further confirmation is required to support the assumption above.

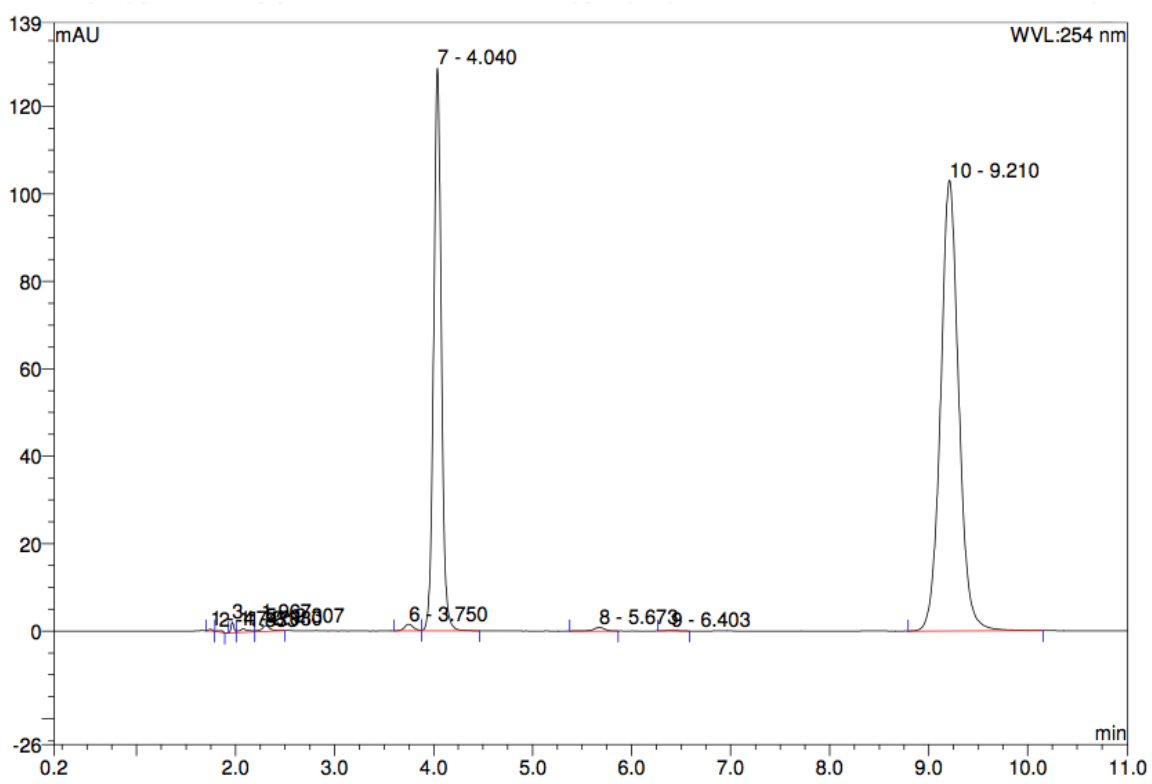

Figure 38. HPLC analysis of activity of 3’-deoxyadenosine. The reaction mixture consisted of 1 mL of 1 mM 3’-deoxyadenosine (cordycepin) in 1 M Tris pH 7.2+ 25 µL of purified enzyme (adenosine nucleosidase from Alaska pea seeds). After 10 hours, the chromatogram shows nucleoside (9.2 minutes), base (4.0 minutes).

CHAPTER IV

CONCLUSION

Nucleoside hydrolases are a family of enzymes that catalyze the hydrolysis of the N-glycosidic bond in purine and pyrimidine nucleosides producing the corresponding base and a ribose. Adenosine nucleosidase, a nucleoside hydrolase, catalyzes the irreversible hydrolysis of the glycosidic bond in adenosine producing adenine and ribose. This enzyme is part of the purine and pyrimidine salvage pathway and allows the reuse of the base without the energy expenditure necessary to synthesize the base *de novo*. Although nucleoside hydrolases have been studied extensively in parasitic protozoans, little information is available on the structure of these enzymes from plants.

Adenosine nucleosidase has been purified from Alaska pea seeds. It demonstrated its highest activity 5 days after germination. A 4-fold purification has been reached with a 1.3 % recovery. The subunit molecular weight was determined by mass spectrometry to be 26,103 daltons. The Michaelis constant, K_m, and the maximum velocity, V_{max}, using adenosine as a substrate were determined to be 137 ± 48 μM, and 0.34 ± 0.02 μM/min respectively.

Based on the reported substrate specificity, the purified enzyme hydrolyzed both purine and pyrimidine nucleosides, which means it belongs to the non-specific inosine-uridine nucleoside hydrolases (IU-NHs). A distinction of this enzyme is that it reacts with 2', 3', and 5'-deoxyadenosine. Although adenosine nucleosidase from other plant sources such as barley leaves, tea leaves, and yellow lupin seeds had a form of deoxyadenosine as

their substrate, the enzyme from Alaska pea seeds was the only one that had 2', 3', and 5'-deoxyadenosine as its substrate. This implies that neither the 2' nor the 3' hydroxyl groups are necessary for the reaction to take place.

This difference becomes evident when the purified enzyme is compared to the nucleoside hydrolases from parasitic protozoans, where deoxynucleosides were not substrates. The substrate specificity of the nucleoside hydrolases for ribose is based on the complex network of interactions that involves the 2', 3' and 5' hydroxyl groups of the sugar and other molecules. This is completely different from the purified enzyme in which the positions of the hydroxyl groups did not affect the activity of the enzyme. Also, this difference indicates that the purified enzyme goes through a different reaction mechanism from that of parasitic protozoans enzymes. This observation is supported by the fact that 3'-deoxyadenosine (cordycepin) is a substrate. This means that, for the purines, it doesn't appear that the hydroxyl group in either the 2' position or in the 3' position is necessary for the reaction. While these results gives a great insight about the enzyme from Alaska pea seeds, further confirmation is required to support the statements above.

REFERENCES

1. Zrenner, R.; Stitt, M.; Sonnewald, U.; Boldt, R. Pyrimidine and Purine Biosynthesis and Degradation in Plants. *Annual Review of Plant Biology* **2006**, 57, pp 805-36.

2. Senecoff, J. F.; McKinney, E. C.; Meagher, R. B. De Novo Purine Synthesis in Arabidopsis Thaliana. II. The PUR7 Gene Encoding 5'-phosphoribosyl-4-(N-succinocarboxamide)-5-aminoimidazole Synthetase Is Expressed in Rapidly Dividing Tissues. *Plant Physiology* **1996**, 112, pp 905-917.

3. Lim, E.; Bowles, D. A Class of Plant Glycosyltransferases Involved in Cellular Homeostasis. *The EMBO Journal* **2004**, 23.15, pp 2915-922.

4. Versees, W.; Steyaert, J. Catalysis by Nucleoside Hydrolases. *Current Opinion in Structural Biology* **2003**, 13, pp 731-738.

5. Petersen, C.; Møller, L. B. The RihA, RihB, and RihC Ribonucleoside Hydrolases of Escherichia Coli. Substrate Specificity, Gene Expression, and Regulation. *The Journal of Biological Chemistry* **2001**, 276.2, pp 884-894.

6. Ogawa, J.; Takeda, S.; Xie, S.; Hatanaka, H.; Ashikari, T.; Amachi, A.; Shimizu, S. Purification, Characterization, and Gene Cloning of Purine Nucleosidase from Ochrobactrum Anthropi. *Applied and Environmental Microbiology* **2001**, 67.4, pp 1783-1787.

7. Kurtz, J.; Exinge, F.; Erbs, F.; Jund, R The URH1 Uridine Ribohydrolase of Saccharomyces Cerevisiae. *Current Genetics* **2002**, 41.3, pp 132-141.

8. Pellé, R.; Schramm, V. L.; Parkin, D. W. Molecular Cloning and Expression of a Purine-specific N-ribohydrolase from Trypanosoma Brucei Brucei. Sequence, Expression, and Molecular Analysis. *The Journal of Biological Chemistry* **1998**, 273, pp 2118-2126.

9. Cui, L.; Rajasekariah, G.; Martin, S. K. A Nonspecific Nucleoside Hydrolase from Leishmania Donovani: Implications for Purine Salvage by the Parasite. *Gene* **2001**, 280, pp 153-162.

10. Ribeiro, J. M.; Valenzuela, J. G. The Salivary Purine Nucleosidase of the Mosquito, Aedes Aegypti. *Insect Biochemistry and Molecular Biology* **2003**, 33.1, pp 13-22.

11. Versées, W.; Holsbeke, E.; De Vos, S.; Decanniere, K.; Zegers, I.; Steyaert, J. Cloning, Preliminary Characterization, and Crystallization of Nucleoside Hydrolases from Caenorhabditis Elegans and Campylobacter Jejuni. *Acta Crystallographica Section D Biological Crystallography* **2003**, 59.6, pp 1087-1089.

12. Liu, X. Characterization of Adenosine Nucleosidase from Yellow Lupin Seeds. Thesis, Middle Tennessee State University, Murfreesboro, TN, 1998.

13. Porcelli, M.; Concilio, L.; Peluso, I.; Marabotti, A.; Facchiano, A.; Cacciapuoti. G. Pyrimidine-specific Ribonucleoside Hydrolase from the Archaeon Sulfolobus Solfataricus – Biochemical Characterization and Homology Modeling. *The FEBS Journal* **2008**, 275.8, pp 1900-1914.

14. Parkin, D. W.; Horenstein, B. A.; Abdulah, D. R.; Estupiia, B.; and Schramm, V. L. Nucleoside Hydrolase from Crithidia Fasciculata. Metabolic Role, Purification, Specificity, and Kinetic Mechanism. *The Journal of Biological Chemistry* **1991**, 226.31, pp 20658-20665.

15. Shi, W.; Schramm, V. L.; Almo, S. C. Nucleoside Hydrolase from Leishmania Major. Cloning, Expression,-catalytic Properties, Transition State Inhibitors, and the 2.5-A Crystal Structure. *The Journal of Biological Chemistry* **1999**, 274.30, pp 21114-21120.

16. Verseaes, W.; Decanniere, K.; Pelle, R.; Depoorter, J.; Brosens, E.; Parkin, D. W.; Steyaert, J. Structure and Function of a Novel Purine Specific Nucleoside Hydrolase from Trypanosoma Vivax. *Journal of Molecular Biology* **2001**, 307.5, pp 1363-379.

17. Parkin, D. W. Purine-specific Nucleoside N-ribohydrolase from Trypanosoma Brucei Brucei. Purification, Specificity, and Kinetic Mechanism. *The Journal of Biological Chemistry* **1996**, 271.36, pp 21713-1719

18. Estupinan, B.; Schramm, V. L. Guanosine-Inosine-preferring Nucleoside N-glycohydrolase from Crithidia Fasciculata. *The Journal of Biological Chemistry* **1994**, 269.37, pp 23068-23073.

19. Degano, M.; Gopaul, D. N.; Scapin, G.; Schramm, V. L.; Sacchettini, J. C. Three-dimensional Structure of the Inosine-uridine Nucleoside N-ribohydrolase from Crithidia Fasciculata. *Biochemistry* **1996**, 35.19, pp 5971-5981.

20. Degano, M.; Almo, S. C.; Sacchettini, J. C.; Schramm, V. L. Trypanosomal Nucleoside Hydrolase. A Novel Mechanism from the Structure with a Transition-state Inhibitor. *Biochemistry* **1998**, 37.18, pp 6277-6285.

21. Miller G. W.; Evans H. J. Nucleosidase from Higher Plants. *Plant Physiology* **1955**, 30.37.

22. Poulton, J. E.; Butt, V. S. Partial Purification and Properties of Adenosine Nucleosidase from Leaves of Spinach Beet (Beta Vulgaris L.). *Planta* **1979**, 131.2, pp 179-185.

23. Guranowski, A.; Schneider, Z. Purification and Characterization of Adenosine Nucleosidase from Barley Leaves. *Biochimica Et Biophysica Acta* **1977**, 482.1, pp 145-158.

24. Imagawa, H.; Yamano, H.; Inoue, K.; Takino, Y. Purification and Properties of Adenosine Nucleosidases from Tea Leaves. *Agricultural and Biological Chemistry* **1979**, 43.11, pp 2337-2342.

25. Chen, C.; Kristopeit, S. K. Metabolism of Cytokinin: Deribosylation of Cytokinin Ribonucleoside by Adenosine Nucleosidase from Wheat Germ Cells. *Plant Physiology* **1981**, 68.5, pp 1020-023.

26. Floch, F. L.; Lafleuriel, J The Purine Nucleosidases of Jerusalem Artichoke Shoots. *Phytochemistry* **1981**, 20.9, pp 2127-2129.

27. Burch, L. R.; Stuchbury, T. Purification and Properties of Adenosine Nucleosidases from Tomato (Lycopersicon Esculentum) Roots and Leaves. *Journal of Plant Physiology* **1986**, 125.3-4, pp 267-273.

28. Abusamhadneh, E. M. Isolation and Characterization of Adenosine Nucleosidase from Yellow Lupin Seeds. Thesis, Middle Tennessee State University, Murfreesboro, TN, 1997.

29. O'Hara, F. The Baran Laboratory. http://www.scripps.edu/baran/images/grpmtgpdf/OHara_Jun_12.pdf (accessed January 2015).

30. Brawerman, G.; Chargaff, E. On a deoxyribonuclease from germinating barley. *J. Biol. Chem.* **1954**, 210, pp 445-454.

31. Fiers, W. , and Vandendriessche, L. Catabolism of nucleosides by barley extracts *Arch. Intern. Physiol. Biochim.* **1960**, 68, pp 203-207.

32. Singhabahu, S.; George, J.; Bringloe, D. Expression of a functional human adenosine deaminase in transgenic tobacco plants. Transgenic Research **2013**, 22, pp643-649.

33. Price, N. C.; Hames, B. D. *Proteins Labfax*. Academic Press and BIOS Scientific Publishers Limited: San Diego, CA and Oxford, UK. 1996.

34. S Sadasivam; A. Manickam. *Biochemical Methods;* New Age International: New Delhi, India. 1996.

35. Altawil, Z. M. Isolation of Nucleoside Metabolizing Enzymes from Alaska Pea Seeds (*Pisum sativum* L. cultivar Alaska). Thesis, Middle Tennessee State University, Murfreesboro, TN, 2013.

36. *The Wolfson Center for Applied Structural Biology*. http://wolfson.huji.ac.il/purification/PDF/IonExchange/GE_IEXcolumns.pdf (accessed March 2015).

37. *GE Healthcare Life Sciences*. http://www.gelifesciences.com/webapp/wcs/stores/servlet/catalog/en/GELifeScie

nces-us/products/AlternativeProductStructure_17468/28936543 (accessed March 2015).

38. Schroder, E.; Jonsson, T.; Poole, L. Hydroxyapatite chromatography: altering the phosphate-dependent elution profile of protein as a function of pH. *Analytical Biochemistry* **2003**, 313, pp 176-178.

39. Lee, W. J.; Pyler, R. E. Nucleic acid degrading enzymes of Barley Malt. III. Adenosine nucleosidase from Malted Barley. *J. Am. Soc.* Brew. Chem., **1986**, 44, pp 86-90.

40. Campos, P.; Rijo-Johansen, M. J.; Carneiro, M. F.; Fevereiro P. Purification and characterization of adenosine nucleosidase from *Coffea Arabica* young leaves. *Phytochemistry*, **2005**, 66, pp 147-151.

41. National Center for Biotechnology Information. PubChem Compound Database; http://pubchem.ncbi.nlm.nih.gov/compound/ (accessed Apr. 6, 2015).

42. Miller, R. L.; Sabourin, C. L. K.; Krenitsky, T. A. Nucleoside hydrolase from *Trypanosoma cruzi*. *J. Biol. Chem.*, **1984**, 259, pp 5073-5077.

43. Parkin, D. W.; Horenstein, B. A.; Abdulah, D. R.; Estupinan, B.; Schramm, V. L. Nucleoside hydrolase from *Crithidia fasciculata*, **1991**, 266, pp 20658-20665.

44. Koszalka, G. W.; Krenitsky, T. A. Nucleoside hydrolase from *Leishmania donovani*. *J. Biol. Chem.*, **1979**, 254, pp 8185-8193.

45. Pelle, R.; Schramm, V. L.; Parkin, D. W. Molecular Cloning and Expression of a Purine-specific N-Ribohydrolase from Trypanosoma brucei brucei. *J. Biol. Chem.*, **1998**, 273, pp 2118-2126.